merry-go-round apparatus with 254-nm light from a low-pressure mercury arc. Samples were purged with nitrogen for 20 min prior to irradiation. Actinometry was carried out by simultaneous irradiation of potassium ferrioxalate solutions.[24] Product yields were determined by GC with conditions appropriate for each sample. In every case except **6f** (*p*-CN), GC response factors for product **7** were determined with acetonitrile solutions of authentic samples of the appropriate derivative of **7**. With **6f** it was assumed that the response factors for **6f** and **7f** were the same as had been shown for the other derivatives of **6**.

Singlet lifetime measurements were carried out in the laboratory of Professor Arthur Halpern of Northeastern University. Samples (in acetonitrile) were excited with 250-270-nm light. Emission was filtered with either a 290-nm interference filter or two CS 0-54 cutoff filters. The flash lamp was a thyratron-driven (12.20 kHz), low-pressure (0.5 Torr) deuterium discharge constructed from platinum electrodes and run at ca. 7 kV. The decay of the lamp was about 0.8 ns. Single exponential decay curves were found for all samples except for the cyano derivatives **6f,g** and **14b**, which had lifetimes too short to allow deconvolution of the curves.

Acknowledgment. We thank Professor Arthur Halpern for his generous help in carrying out the singlet lifetime measurements. This work was supported by grants from the National Science Foundation and the donors of the Petroleum Research Fund, administered by the American Chemical Society.

Photophysics of a Cofacial Porphyrin–Quinone Cage Molecule and Related Compounds: Fluorescence Properties, Flash Transients, and Electron-Transfer Reactions

Jonathan S. Lindsey,*† John K. Delaney,‡ David C. Mauzerall,*‡ and Henry Linschitz§

Contribution from the Department of Chemistry, Carnegie Mellon University, Pittsburgh, Pennsylvania 15213, The Rockefeller University, New York, New York 10021, and Department of Chemistry, Brandeis University, Waltham, Massachusetts 02254.
Received July 28, 1987

Abstract: Fluorescence yields, fluorescence lifetimes, and flash photolysis transients have been measured for a tetrabridged cofacial porphyrin–quinone cage molecule and related derivatives. When the quinone is present and in the oxidized form, two fluorescence lifetimes are observed for the zinc complex, both shorter than the single lifetimes of control compounds. These are assigned to two conformers, with porphyrin to quinone interplanar separation of about 8.5 and 6.5 Å, respectively. The fluorescence lifetime data lead to electron-transfer times for the two conformers of between 0.5 and 15 ns. The fast electron-transfer time is only weakly dependent on solvent and is independent of temperature between 290 and 124 K. Following flash photolysis of the zinc–porphyrin–quinone in polar solvents, a transient band at 415 nm grows in more slowly (150 ns) and decays much more rapidly (1.4 μs) than the triplet seen in control compounds and is assigned to a charge-separated ZnP^+Q^- state. The reaction leading to this state exhibits an activation energy of only 6 kJ/mol. In contrast to the zinc chelate, the free base porphyrin–quinone shows no electron-transfer interactions. These results support a distance-sensitive nonadiabatic electron-tunneling mechanism for the transfer. Effects of solvent and protonation are interpreted in terms of conformational changes that modify the porphyrin–quinone distance. Attempts to study effects of orbital symmetry in a pair of chlorin–quinones were inconclusive. A larger fraction of energy is stored in forming the charge-separated state (1.4 eV, ΔG) from the triplet state (1.6 eV, ΔE) of the zinc–porphyrin–quinone than is stored in the bacterial reaction center (0.5 eV) from the singlet state (1.2 eV).

Electron-transfer reactions make possible the complex flow of energy in biological systems and are receiving increasing attention as the initial step in many chemical reactions. One of the most dramatic examples of energy flow via electron transfer occurs in the reaction centers of photosynthetic systems. These assemblies function with quantum yields greater than 95%, a maximum photon energy conversion efficiency of 30–50%, and are sufficiently robust and channeled to maintain function after $>10^7$ cycles. Understanding the determinants of such fast, efficient, and stable electron-transfer reactions remains a central challenge in chemistry.

A variety of studies involving temperature and transfer distance have shown that the primary reactions in photosynthesis involve electron–nuclear tunneling.[1] For example, the initial electron-transfer events in intact reaction centers occur at 4 K,[2] and the reverse electron transfer, from quinone to bacteriochlorophyll, has the remarkably low activation energy of $<1.7 \times 10^{-3}$ kJ/mol between 80 and 1.4 K.[3] Recent X-ray crystallographic structure determination has shown the minimum edge-to-edge distance of the reacting pigments to be >5 Å.[4] Thus, the electron-transfer reactions occur at distances greater than the sum of the van der Waals contact radii. This latter feature in particular is characteristic of electron tunneling and sharply distinguishes these reactions from the slow adiabatic electron-transfer reactions characteristic of more common redox processes.

Electron tunneling, a basic quantum mechanical phenomenon, is not restricted to the highly ordered photosynthetic structures but is observed in systems of widely varying complexity.[5] Photoinduced electron-transfer reactions of porphyrins in solution occur at an "encounter radius" of 20 ± 2 Å, much greater than the sum of the radii of the porphyrin macrocycles.[6] Photoexcited

† Carnegie Mellon University.
‡ The Rockefeller University.
§ Brandeis University.

(1) DeVault, D. *Quantum-Mechanical Tunnelling in Biological Systems*; Cambridge University: Cambridge, U.K., 1984.
(2) Arnold, W.; Clayton, R. K. *Proc. Natl. Acad. Sci. U.S.A.* **1960**, *46*, 769–776.
(3) McElroy, J. D.; Mauzerall, D. C.; Feher, G. *Biochim. Biophys. Acta* **1974**, *333*, 261–277.
(4) Deisenhofer, J.; Epp, O.; Miki, K.; Huber, R.; Michel, H. *Nature (London)* **1985**, *318*, 618–624.
(5) Khairutdinov, R. F.; Brickenstein, E. Kh. *Photochem. Photobiol.* **1986**, *43*, 339–356.
(6) Ballard, S. G.; Mauzerall, D. In *Tunneling in Biological Systems*; Chance, B., DeVault, D., Eds.; Academic: New York, 1979, pp 581–587. Carapellucci, P. A.; Mauzerall, D. *Ann. N.Y. Acad. Sci.* **1975**, *244*, 214–238.

0002-7863/88/1510-3610$01.50/0

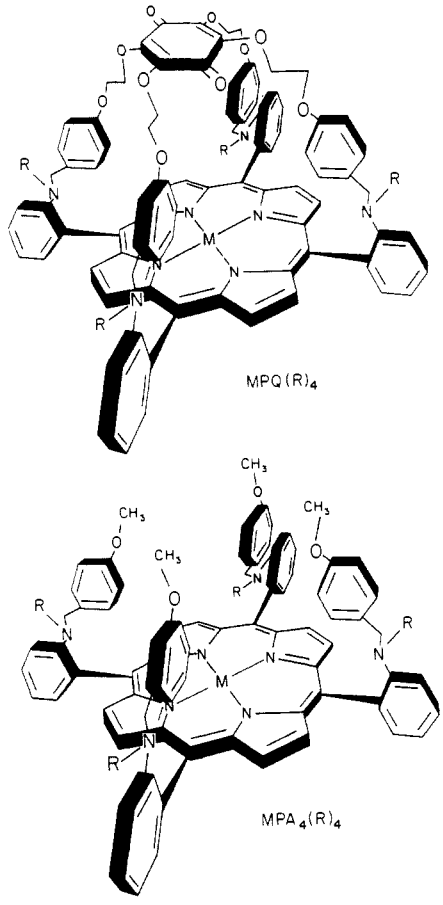

Figure 1. Family of free base (M = H_2) and zinc (M = Zn) porphyrin compounds. The free base porphyrin–quinone with four benzylaniline groups (R = H) as spacers is designated by the shorthand PQ; the zinc chelate, ZnPQ. Modification of the amines in the spacer units is denoted by parentheses: the acetylated (R = Ac) zinc–porphyrin–quinone derivative, $ZnPQ(Ac)_4$; the protonated (R = H_2^+) derivative, $ZnPQ(H^+)_4$; when the amines are in Schiff base linkages rather than benzylanilines, $ZnPQ(SB)_4$. Two compounds that do not undergo intramolecular electron transfer are used as controls. Reduction of the quinone in PQ gives the porphyrin hydroquinone (PQH_2), and the tetraanisylporphyrin derivative (PA_4) has similar substituents but no quinone. The shorthand for substitution of the amines in the spacer units is identical for PQ and PA_4.

porphyrins react in nanosecond times with acceptors across the bilayer lipid membrane–aqueous interface.[7] Photoproduced reductants on the surface of cytochromes react with hemes at a distance of 15 Å.[8] The decay of ions in organic glasses occurs via long-distance electron-transfer reactions.[9] Although some of these studies of electron transfer at a distance in solutions, solids, and at interfaces provide powerful evidence for a mechanism involving electron tunneling, it is clearly desirable to work with synthetic systems combining donor and acceptor moieties held in controlled three-dimensional geometries. Such models permit study of the important structural parameters of distance, orientation, and symmetry, the environmental contributions of media polarity, polarizability, and point charges, and temperature dependence. Experimental data regarding these parameters are needed to understand the basis of efficient electron transfer in photosynthesis as well as in the action of redox enzymes.[10]

Nevertheless, although over 25 model compounds containing porphyrin and quinone components have been synthesized, few such comprehensive photochemical studies have been performed.[11] This paper describes an investigation of most of these effects on excited-state donor–acceptor interactions in a small family of porphyrin–quinone cage molecules.

Molecular Design. The structures of the porphyrin–quinone and derivatives in this photochemical study are shown in Figure 1. The essential structural elements consist of porphyrin, quinone, and four intervening spacer units. The function of the spacers is to enforce a cofacial geometry and prevent direct intramolecular van der Waals contact of the porphyrin and quinone. The cofacial geometry was chosen in order to maximize orbital overlap of the porphyrin and quinone.[12] The porphyrin–quinone distance was designed to be near the expected optimum in the yield–lifetime product of charge separation.[12]

The nature of the intervening spacer units could be modified in four possible ways by alteration of the *o*-amino groups. The cage molecule was constructed in one step and in high yield by the equilibrium condensation of *meso*-$\alpha,\alpha,\alpha,\alpha$-tetrakis(*o*-aminophenyl)porphyrin with the quinone tetrabenzaldehyde, forming the tetrakis(Schiff base) product $PQ(SB)_4$.[13] Reduction of the Schiff bases with $NaBH_3CN$ gave the porphyrin–quinone (PQ) containing benzylaniline moieties in the spacer units. The structure was further varied by acetylation of the benzylanilines in ZnPQ to form the amides $ZnPQ(Ac)_4$ and protonation of the benzylanilines with strong acids to form anilinium cations $ZnPQ(H^+)_4$.

The tetraalkoxyquinone in the PQ structure resembles ubiquinone, a 2,3-dimethoxy-5-methyl-6-alkyl-1,4-benzoquinone that functions as the secondary electron acceptor in the photosynthetic reaction center. Quinone reduction potentials vary enormously with substitution,[14] and both ubiquinone ($E_{1/2}$ = −0.70 V vs SCE)[15] and tetraalkoxyquinones ($E_{1/2}$ = −0.667 V vs SCE; see Experimental Section) are difficult to reduce because of the electron-releasing nature of their alkyl and alkoxy substituents.

The free base porphyrins can be converted easily to the corresponding zinc chelates. Zinc porphyrins exhibit general photochemical features resembling that of chlorophyll but are less susceptible to adventitious demetalation than are the magnesium chelates. Zinc porphyrins also undergo reversible electrochemistry, form stable radical cations, and are better reductants in the excited states than the free base porphyrins.

The photochemical features of the porphyrin–quinones are compared with two structurally related reference compounds where intramolecular electron-transfer reactions cannot occur (Figure 1). The tetraanisylporphyrin (PA_4) bears the same substituents as the porphyrin–quinone (PQ) but lacks the quinone. Reduction of the quinone in PQ gives the porphyrin–hydroquinone (PQH_2).

Results

Our results are presented in the following manner. We first describe the absorption spectra of the porphyrin–quinones, which distinguish amine–porphyrin charge-transfer interactions from the porphyrin–quinone photoinduced charge-separation processes. Discussion of the solution conformations of PQ and a kinetic

(7) Hong, F. T.; Mauzerall, D. *J. Electrochem. Soc.* **1976**, *123*, 1317–1324. Woodle, M.; Zhang, J. W.; Mauzerall, D. *Biophys. J.* **1987**, *52*, 577–586.
(8) Mayo, S. L.; Walther, R. E.; Crutchley, R. J.; Gray, H. B. *Science (Washington, D.C.)* **1986**, *233*, 948–952.
(9) Miller, J. R. *Chem. Phys. Lett.* **1973**, *22*, 180–182. Miller, J. R. *J. Phys. Chem.* **1975**, *79*, 1070–1078. Miller, J. R. *Science (Washington, D.C.)* **1975**, *189*, 221–222. Miller, J. R.; Beitz, J. V.; Huddleston, R. K. *J. Am. Chem. Soc.* **1984**, *106*, 5057–5068.
(10) Kuki, A.; Wolynes, P. G. *Science (Washington, D.C.)* **1987**, *236*, 1647–1652.
(11) For a review, see: Boxer, S. G. *Biochim. Biophys. Acta* **1983**, *726*, 265–292. For comprehensive recent lists of porphyrin–quinone references, see: Gust, D.; Moore, T. A.; Liddell, P. A.; Nemeth, G. A.; Makings, L. R.; Moore, A. L.; Barrett, D.; Pessiki, P. J.; Bensasson, R. V.; Rougée, M.; Chachaty, C.; De Schryver, F. C.; Van der Auweraer, M.; Holzwarth, A. R.; Connolly, J. S. *J. Am. Chem. Soc.* **1987**, *109*, 846–856, ref 12. Sanders, G. M.; van Dijk, M.; van Veldhuizen, A.; van der Plas, H. C. *J. Chem. Soc., Chem. Commun.* **1986**, 1311–1313, ref 1. Morgan, B.; Dolphin, D. *Angew. Chem., Int. Ed. Engl.* **1985**, *24*, 1003–1004, ref 2.
(12) Mauzerall, D. *Brookhaven Symp. Biol.* **1976**, *No. 28*, 64–73. Mauzerall, D. In *The Porphyrins*; Dolphin, D., Ed.; Academic: New York, 1978; Vol. V, pp 29–52.
(13) Lindsey, J. S.; Mauzerall, D. C. *J. Am. Chem. Soc.* **1982**, *104*, 4498–4500.
(14) Patai, S. *The Chemistry of The Quinonoid Compounds*; Wiley: New York, 1974; Vol. I, II.
(15) Morrison, L. E.; Schelhorn, J. E.; Cotton, T. M.; Bering, C. L.; Loach, P. A. In *Function of Quinones in Energy Conserving Systems*; Trumpower, B. L., Ed., Academic: New York, 1982; pp 35–58.

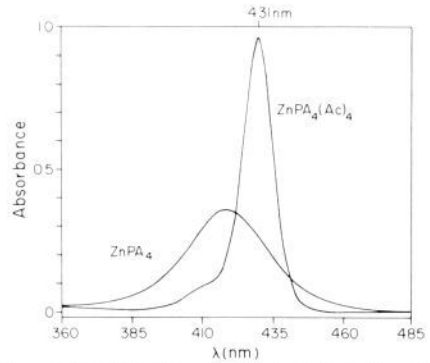

Figure 2. Sharpening of the Soret band upon acetylation of each of the amines in $ZnPA_4$ to give $ZnPA_4(Ac)_4$. The fwhm decreases from 27 to 10 nm, the ϵ_{Soret} increases from 172 000 to 455 000 M^{-1} cm^{-1} (conservation of transition strength), and the λ_{max} shifts from 419 to 431 nm. The porphyrin visible bands (not shown) undergo a 5–10-nm red shift but are unchanged in both intensity and fwhm upon acetylation. The same phenomena are observed with ZnPQ. Nearly identical changes in the absorption spectrum also occur upon protonation of the amines, forming $ZnPQ(H^+)_4$ and $ZnPA_4(H^+)_4$. The tetra-Schiff base porphyrin–quinone $ZnPQ(SB)_4$ also has a normally sharp Soret band.

scheme provides the framework for understanding the overall photochemical features of the porphyrin–quinones. We then summarize the fluorescence measurements of the zinc derivatives, including solvent and temperature dependencies, and the related flash photolysis observations on triplet-state reactions. Next, the free base porphyrin–quinones are shown to be unreactive. Finally, the effects of symmetry and charge are described via the fluorescence properties of chlorin–quinone structural isomers and the protonated zinc–porphyrin–quinone.

General Features. (1) Spectra. Tetraphenylporphyrins with *o*-amino substituents have strikingly broadened Soret bands (PQ, 40 nm fwhm) and lowered peak extinctions (PQ; ϵ 124 400 M^{-1} cm^{-1}) compared with that of tetraphenylporphyrin (TPP, 10 nm fwhm and $\epsilon \sim 500\,000$ M^{-1} cm^{-1}), but the transition moment is conserved (Figure 2). The extent of Soret broadening is proportional to the number of amino groups, increases with amine basicity, and decreases on going from the free base to the zinc chelate (see Experimental Section). In contrast to the Soret broadening, the visible absorption bands of these compounds are nearly identical with those of unsubstituted tetraphenylporphyrins. The fluorescence emission spectra undergo changes in the ratios of the two emission bands upon substitution but otherwise are unaffected (see Experimental Section).

The Soret broadening is abolished in those chemical modifications that lower the energy of the amine lone pair. Acetylation, protonation, and Schiff base formation all cause a dramatic sharpening of the Soret band (Figure 2). These effects are identical for both the PQ and PA_4 compounds and hence are independent of the presence of the quinone.

We attribute this broadening of the Soret to a charge-transfer interaction of the amine lone pair of electrons with the second excited state of the porphyrin, the transition to which is strongly allowed. The visible absorption and fluorescence bands, which derive from forbidden transitions to and from the first excited state of the porphyrin, are unaffected by the presence of *o*-amines. Similar observations have been made on other weak charge-transfer complexes of porphyrins.[16]

The absorption spectrum of the acetylated Zn–porphyrin–quinone $ZnPQ(Ac)_4$ is equal to the sum of the component chromophores. No charge-transfer bands appear in the UV–visible absorption spectrum. The porphyrin dominates the visible absorption spectrum, and the quinone contributes strongly ($\epsilon \sim$ 16 000 M^{-1} cm^{-1}) only at 300 nm. The quinone also absorbs broadly at 400 nm, but the intensity is extremely weak ($\epsilon \sim 200$ M^{-1} cm^{-1})[17] versus the Zn–porphyrin ($\epsilon \sim 10^5$ M^{-1} cm^{-1}). The

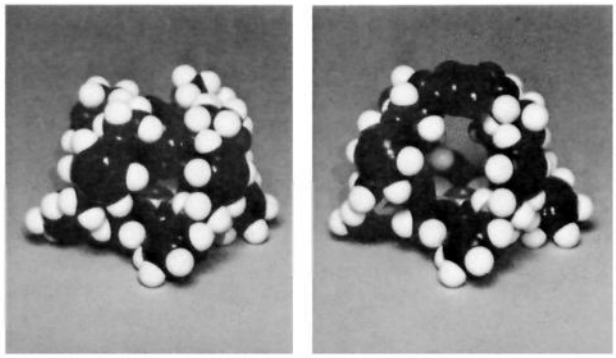

Figure 3. Space-filling models of the PQ conformers. The helical twisting of the four spacer groups occurs in both conformers, rotating the quinone carbonyl axis about 45° with respect to the N–N symmetry axes of the porphyrin. The different conformations of the dioxyethylene moieties in PQ_a (left) and PQ_b (right) give P–Q distances of about 6.5 and 8.5 Å, respectively. The conformers do not equilibrate within the porphyrin fluorescence lifetime (2 ns) but are equilibrated on the 1-μs time scale.

acetanilide moieties absorb in the far-UV and contribute only weakly at 280 nm ($\epsilon \sim 530$ M^{-1} cm^{-1}), again less than the zinc–porphyrin ($\epsilon \sim 10\,000$ M^{-1} cm^{-1}).

(2) Oxidation Properties. We sought to obtain the absorption spectrum of the radical cation of ZnPQ for use as a reference in flash photolysis experiments. Chemical oxidation of ZnPQ with $Fe(ClO_4)_3$ in acetonitrile resulted in a broad featureless absorption spectrum rather than the distinct band at 409 nm found with ZnTPP.[18] Furthermore, this oxidation was not reversed by triethylamine, suggesting destructive oxidation of the benzylaniline moieties. Chemical oxidation by $Fe(ClO_4)_3$ of $ZnPQ(Ac)_4$ resulted in a similar broad absorption spectrum. However, addition of triethylamine regenerated the absorption spectrum of the closed-shell species $ZnPQ(Ac)_4$. The reversibility of the oxidation–reduction process in $ZnPQ(Ac)_4$ resembles that of ZnTPP and illustrates the electrochemical stability of the amide linkages in the spacer units of $ZnPQ(Ac)_4$ (see Experimental Section for potentials). Therefore, most photochemical studies were performed on the acetylated porphyrin derivatives.

(3) Molecular Structure. We have previously published data showing that $ZnPQ(Ac)_4$ exhibits biphasic fluorescence decay curves.[19] The occurrence of two lifetimes has been observed in every zinc–porphyrin–quinone of this family, including ZnPQ, $ZnPQ(Ac)_4$, and $ZnPQ(SB)_4$, suggesting the presence of two molecular conformers of the porphyrin–quinone molecule. Crystals of PQ of sufficient quality for an X-ray diffraction study were not obtained. A detailed solution-phase NMR study was performed on the free base porphyrin–quinone with the following conclusions.[20]

The solution average structure of PQ consists of the four spacer units twisted in a spiral array similar to strands in a rope, causing two major effects on the overall PQ structure. First, the carbonyl axis of the quinone is rotated approximately 45° with respect to the N–N symmetry axes of the porphyrin. Second, the cage molecule is partially collapsed, causing the porphyrin–quinone interplanar distance of separation to be less than the 10 Å expected with all four spacer units in full upright positions.[19] Despite the compact nature of the cage, molecular models show that the cavity is still large enough to accommodate small solvent molecules.

The PQ molecule in solution is a dynamic entity. The phenylene rings in the spacer units rotate about their para axis; the rotation is rapid on the NMR time scale and is not frozen out at −75 °C

(16) Mauzerall, D. *Biochemistry* **1965**, *4*, 1801–1810.

(17) Flaig, W.; Salfeld, J. C. *Justus Liebigs Ann. Chem.* **1958**, *618*, 117–139.

(18) Fajer, J.; Borg, D. C.; Forman, A.; Dolphin, D.; Felton, R. H. *J. Am. Chem. Soc.* **1970**, *92*, 3451–3459.

(19) Lindsey, J. S.; Mauzerall, D. C.; Linschitz, H. *J. Am. Chem. Soc.* **1983**, *105*, 6528–6529.

(20) Lisicki, M. A.; Mishra, P. K.; Bothner-By, A. A.; Lindsey, J. S. *J. Phys. Chem.*, in press.

Table I. Fluorescence Yields and Lifetimes of Zinc Porphyrins[a]

compd	rel ϕ_f[b]	τ_1	τ_2	χ_1	$k_f/10^7$,[c] s^{-1}
ZnTPP	1.0	1.86		1.0	2.2
ZnPQ	0.35	0.6	1.8	0.55	1.6
$ZnPA_4$	0.86	3.0		1.0	1.2
$ZnPQH_2$	0.86	2.5		1.0	1.4
$ZnPQ(Ac)_4$	0.28	0.5	1.3	0.60	1.7
$ZnPA_4(Ac)_4$	0.68	2.2		1.0	1.2
$ZnPQH_2(Ac)_4$	0.68	2.2		1.0	1.2
$ZnPQ(SB)_4$	0.28	0.4	2.1	0.60	1.9

[a] In acetonitrile at room temperature. The τ values are in nanoseconds. [b] Total integrated fluorescence emission (610 and 660 nm). [c] The fluorescence rate constants were calculated by taking the absolute fluorescence yield of ZnTPP to be 0.04.[64]

in CD_2Cl_2. The helical twisting of the four spacer units can occur equally to the right or to the left, and the clockwise and counterclockwise twisted PQ molecules interconvert through an upright configuration. Because the porphyrin and quinone distance of separation and relative orientations are identical in these two twisted structures, it is expected that their photochemical properties would be identical. Space-filling molecular models indicate that two distinct and difficultly interconvertible conformations of the oxyethyleneoxy moieties in the PQ molecule can occur, resulting in an introverted and an extroverted structure with porphyrin–quinone center-to-center distances of about 6.5 and 8.5 Å, respectively (Figure 3). In both conformers the oxyethyleneoxy moieties in the spacer groups are in gauche configurations, consistent with but indistinguishable by the NMR data. The two fluorescence lifetimes are thus attributed to the twisted introverted PQ conformer (PQ_a) with shorter P–Q distance, which readily undergoes electron transfer, and the twisted extroverted PQ conformer (PQ_b), which undergoes electron transfer with longer lifetime. The description of the porphyrin–quinone as a two-state system is adequate to explain the photochemical data.

Photochemical Scheme. The photophysical properties of the zinc–porphyrin–quinones are conveniently described with the aid of Scheme I, which involves the two conformers PQ_a and PQ_b. The initial excited state of each conformer is presumed to undergo very fast relaxation to its respective lowest excited singlet level, because the observed properties are independent of excitation energy, whether above the Soret band or into the visible bands. Assuming the two conformers do not interconvert within the 2-ns lifetime of the excited zinc–porphyrin, the initial relative amplitudes of the short and long lifetime represent the relative amounts of the introverted and extroverted conformers, respectively. The ^1PQ states can fluoresce (k_f), undergo internal conversion to the triplet state ^3PQ (k_{isc}), or decay to the ground state (k_{ic}). If and only if the quinone is present and in the oxidized form, electron transfer to $^1P^+Q^-$ can occur via k_a and k_b. This charge-transfer state can decay to the ground state (k_3, k_3'). The triplet state also undergoes electron transfer (k_4) to form $^3P^+Q^-$, which in turn decays to the ground state (k_5).

Scheme I

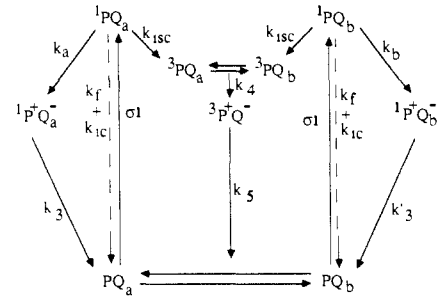

The fluorescence as a function of time, following δ-function excitation is given by

$$F(t) = k_f[^1PQ_a \exp(-k_1 t) + {}^1PQ_b \exp(-k_2 t)] \quad (1)$$

where

$$^1PQ_a + {}^1PQ_b = {}^1PQ \qquad \chi_1 = {}^1PQ_a/{}^1PQ \quad (2)$$

$$1/\tau_1 = k_1 = k_f + k_{ic} + k_{isc} + k_a = k_0 + k_a \quad (3)$$

$$1/\tau_2 = k_2 = k_f + k_{ic} + k_{isc} + k_b = k_0 + k_b \quad (4)$$

Because the absorption spectrum of each porphyrin–quinone compound is the sum of its components, the interaction of the porphyrin and the quinone must be weak, and we take k_f, k_{ic}, and k_{isc} to be the same for both conformers ($k_0 = k_f + k_{ic} + k_{isc}$). The differences in both fluorescence yield and lifetime are assigned to differences in k_a and k_b.

For the case of $ZnPQH_2(Ac)_4$ or $ZnPA_4(Ac)_4$, there will be only one lifetime:

$$1/\tau_0 = k_0 = k_f + k_{ic} + k_{isc} \quad (5)$$

The fluorescence yield of $ZnPQ(Ac)_4$ relative to $ZnPQH_2(Ac)_4$ is

$$\phi(\text{rel}) = \frac{\phi(ZnPQ(Ac)_4)}{\phi(ZnPQH_2(Ac)_4)} = {}^1PQ_a\frac{k_0}{k_1} + {}^1PQ_b\frac{k_0}{k_2} \quad (6)$$

The quantum yield of charge transfer produced from the singlet state in polar solvents is

$$^1\phi_{ET} = \chi_1 k_a/k_1 + (1 - \chi_1)k_b/k_2 \quad (7)$$

Assuming k_0 of $ZnPQ(Ac)_4$, $ZnPQH_2(Ac)_4$, and $ZnPA_4(Ac)_4$ to be the same, one can obtain k_a and k_b by combining fluorescence lifetime data of these compounds (Tables I and II). The same analysis can be performed among porphyrins bearing similar substituents, such as ZnPQ and $ZnPA_4$.[21]

Table II. Fluorescence Yields and Lifetimes as Function of Solvent[a]

	$ZnPQ(Ac)_4$			$\phi_f(ZnPQ(Ac)_4)/\phi_f(ZnPA_4(Ac)_4)$			$ZnPA_4(Ac)_4$	
solvent	τ_1	τ_2	χ_1	measd	calcd	$k_f/10^7$	τ_1	rel ϕ_f[e]
toluene	1.0	2.5	0.5	0.85	0.93	1.2	2.1	1.0
ethyl acetate	1.1	2.0	0.5	0.63	0.70	1.2	2.1	0.9
THF[b]	0.9	1.9	0.6	0.60	0.59	1.4	2.1	0.95
CH_2Cl_2	1.16	1.9	0.58	0.55	0.67	1.1	2.18	0.88
pyridine	0.5	2.1	0.8	0.39	0.37	1.8	2.1	0.94
ethanol	0.5	2.1	0.85	0.29	0.34	1.4	2.1	0.98
acetonitrile	0.5	1.3	0.6	0.42	0.37	1.7	2.05	0.86
DMAC[c]	0.45	2.1	0.8	0.32	0.35	1.6	2.1	0.93
DMSO[d]	0.5	2.1	0.85	0.29	0.34	1.4	2.1	0.97

[a] At room temperature with excitation wavelength 337 nm and emission measured at both 614 and 660 nm. The average value (spread ±5%) is reported. The values of τ are in nanoseconds. [b] Tetrahydrofuran. [c] *N,N*-Dimethylacetamide. [d] Dimethyl sulfoxide. [e] Normalized to $ZnPA_4(Ac)_4$ in toluene.

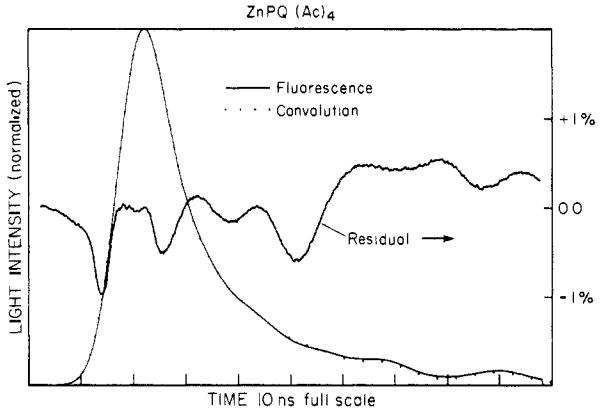

Figure 4. Fluorescence lifetime of $ZnPQ(Ac)_4$ in acetonitrile at room temperature (emission 660 nm). The laser pulse was convoluted with two exponentials [τ 0.4, 1.3 ns (60:40)] to curve fit the observed decay. The residual is the difference between the observed and convoluted profiles.

Table III. Electron-Transfer Time Constants

compd[a]	τ_a	τ_b[b]	$K = \chi_1/(1-\chi_1)$
ZnPQ	0.88	6	1.2
$ZnPQ(Ac)_4$	0.65	3	1.5
$ZnPQ(SB)_4$	0.50	>30	1.5

	$ZnPQ(Ac)_4$			
solvent	τ_a	τ_b	K	τ_b/τ_a
toluene	1.7	≥20	1.0	
ethyl acetate	2.0	10	1.0	5
tetrahydrofuran	1.4	8	1.5	5.7
CH_2Cl_2	2.1	8	1.3	3.8
pyridine	0.62	13	4.0	21
ethanol	0.62	13	5.6	21
acetonitrile	0.62	3	1.5	4.8
DMAC[c]	0.55	13	4.0	24
dimethyl sulfoxide	0.62	13	5.6	21

[a] In acetonitrile. [b] The closeness of the measured value of τ_2 to τ_0 results in large errors in τ_b. Calculations of τ_a and τ_b were performed using τ_0 = 2.5 ns.[65] All τ values are in nanoseconds. [c] *N,N*-Dimethylacetamide.

Fluorescence Properties of Zinc–Porphyrins. The fluorescence yields and lifetimes (Figure 4) of a family of systematically modified zinc–porphyrin–quinones are given in Table I. Low yields of fluorescence and biphasic fluorescence lifetimes are found only in those cases where quinone is both present and in the oxidized form. These low yields are therefore attributed to an excited-state charge-transfer reaction forming a P^+Q^- charge-separated state. The three molecules, ZnPQ, $ZnPQ(Ac)_4$, and $ZnPQ(SB)_4$, behave similarly, indicating that ortho substitution does not alter the two conformers. Expressed as reciprocal rate constants, the electron-transfer time constants of the conformers ^1PQ_a and ^1PQ_b of $ZnPQ(Ac)_4$ are listed in Table III. The fluorescence yields calculated from these rate constants on the above assumptions (eq 6) are in good agreement with measurement (Tables I, II). The value of k_f changes little [$(1.46 \pm 0.26) \times 10^7$ s^{-1}] among these compounds, illustrating the consistency of this analysis. For $ZnPQ(Ac)_4$ in polar solvents the quantum yield of singlet-state charge transfer is 0.60 (eq 7).

(21) Analysis of the complete set of equations, which includes rate constants for equilibration of the two conformers, brings out the limits. If the interconversion is rapid relative to the lifetimes, then only a single exponential will be observed. If the interconversion constants are greater than the other rate constants, then the ratio of the amplitudes of the fast to that of the slow observed exponentials (which we call K) will always be <1. Since we often observe $K > 1$ (Tables III and IV), the interconversion rate must be slower than the decay rates. Expansion of the quadratic for this case shows that the fast-decay constant is at most the sum of the electron-transfer rate constant k_a plus the sum of the interconversion constants while the slow-decay constant is k_b plus one of these constants times a factor that goes to zero as K goes to one.

Table IV. Fluorescence and Electron-Transfer Times of $ZnPQ(Ac)_4$ as a Function of Temperature[a]

temp, K	τ_1	τ_2	τ_a	τ_b	$K = \chi_1/(1-\chi_1)$
290	0.54	1.6	0.69	4	2.45
265	0.59	2.3	0.77	*b*	2.03
245	0.61	2.5	0.80	*b*	2.57
219	0.55	1.8	0.70	6	1.56
165	0.8	2.1	1.2	13	0.69
124	0.6	2.4	0.8	*b*	0.27
ΔE, kJ/mol			0.0 ± 1.2	~4 ± 2	
ΔH, kJ/mol					3.7 ± 0.8

[a] In *N,N*-dimethylacetamide/ethanol (1:1). Excitation wavelength was 337 nm, and emission was measured at both 614 and 660 nm. The average value is reported. All τ values are in nanoseconds. [b] The closeness of the measured value of τ_2 to τ_0 results in large errors in τ_b. Calculations of τ_a and τ_b were performed using τ_0 = 2.5 ns.[65]

In several cases the lifetimes were verified to be independent of concentration (10^{-7}–10^{-5} M), excitation wavelength [337 nm (N_2 laser) or 565 nm (N_2-pumped rhodamine dye laser)], and emission wavelength (614 nm or 660 nm, using interference filters). To determine if two different porphyrin excited states might be responsible for the two fluorescence lifetimes,[19] dynamic fluorescence polarization experiments were performed on ZnPQ using sucrose octaacetate[22] as a room temperature rigid (nanosecond time range) solvent. The fluorescence lifetimes were identical (τ_1 1.09 ns, τ_2 2.0 ns, χ_1 0.71) at both 614 and 660 nm with both parallel and perpendicular polarization. The maximum polarization (λ_{ex} 610 nm, λ_{em} 660 nm) observed with ZnPQ (+0.05) was less than that of ZnTPP (+0.15, planar oscillator). The polarization was constant throughout the fluorescence decay, with no observable splitting of the 4-fold symmetry of the porphyrin by the quinone.

The fluorescence yields and lifetimes of $ZnPQ(Ac)_4$ in various solvents generally decrease with increasing polarity of the solvent (Table II). In contrast, the single lifetime of $ZnPA_4(Ac)_4$ is independent of solvent, changing less than 15% over the entire range of solvent polarity. The increase of electron-transfer time with decreasing polarity of solvent is rather mild for conformer a and occurs only at a dielectric constant <10 (Table III). The effect of solvent is harder to discern in conformer b, partly because of the uncertainty in τ_b. An exceptional solvent is acetonitrile, which gives a shorter τ_b and a smaller fraction of the PQ_a conformer than other polar solvents. The ratio of the two conformers also changes with solvent, from 1:1 in toluene to 5.6:1 in dimethyl sulfoxide, in favor of conformer PQ_a.

The temperature dependence of electron transfer from the singlet state is given in Table IV for $ZnPQ(Ac)_4$ in *N,N*-dimethylacetamide/ethanol (1:1). The fluorescence decays for the two emission wavelengths were nearly identical at each temperature. The electron-transfer time for conformer PQ_a is temperature independent from 290 to 124 K (ΔE = 0.0 ± 1.2 kJ/mol), while that for conformer PQ_b may increase on cooling with a small activation energy of 4 ± 2 kJ/mol. [The equilibrium constant ($K = PQ_a/PQ_b$) of the two conformers shifts to favor PQ_b as the temperature decreases, with an enthalpy of 4 kJ/mol for the reaction $PQ_b \rightarrow PQ_a$.]

Flash Transients of Zinc–Porphyrins. Preliminary flash photolysis studies on the reaction of the triplet state have been published.[19] Flash photolysis of $ZnPQH_2(Ac)_4$ and $ZnPA_4(Ac)_4$ using a frequency-doubled pulsed ruby laser gave transients (Figure 5) identified as triplet states by their lifetimes ($\tau > 10^{-4}$ s), spectra,[24] and quenching by oxygen. The formation of the triplet state occurred within the response time (30 ns) of the instrument.[25] $ZnPQ(Ac)_4$ gave quite different results. In polar

(22) Domingue, R. P.; Fayer, M. D. *J. Chem. Phys.* **1985**, *83*, 2242–2251.
(23) Delaney, J. K.; Mauzerall, D. C.; Lindsey, J. S., manuscript in preparation.
(24) Pekkarinen, L.; Linschitz, H. *J. Am. Chem. Soc.* **1960**, *82*, 2407–2411.

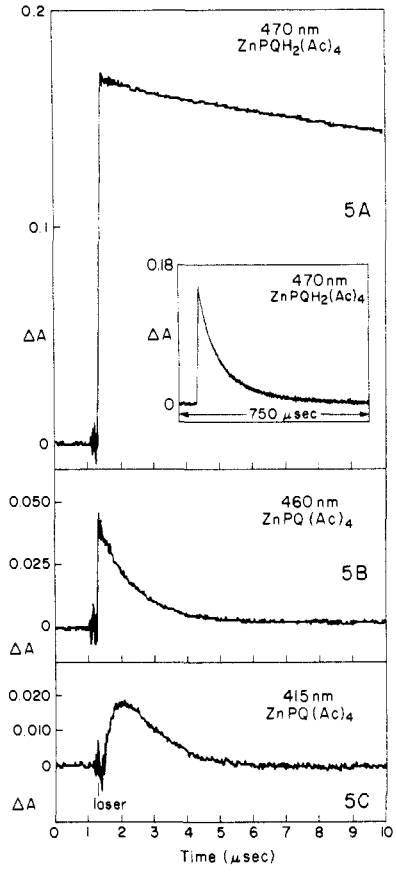

Figure 5. Flash photolysis transients of $ZnPQ(Ac)_4$ and $ZnPQH_2(Ac)_4$ at 5×10^{-5} M in CH_3CN/ethanol (3:1) at room temperature. The tetraacetylated zinc–porphyrin–hydroquinone $ZnPQH_2(Ac)_4$ shows (470 nm) the long-lived triplet state with lifetime limited by triplet–triplet quenching (5A). With $ZnPQ(Ac)_4$ at 415 nm (5C), an isosbestic point of the triplet and ground states, a growing in is observed with rise time of 150 ns and decay of 1.4 μs. This is assigned to intramolecular charge separation, giving $ZnP^+Q^-(Ac)_4$. At other wavelengths (460 nm) where the cation and triplet absorb equally, a rapid rise limited by the response time (30 ns) of the apparatus[25] is observed (5B). The transients observed at all wavelengths decay with a lifetime of 1.4 μs (5B,C). The quantitative reversibility of the charge separation is indicated by the return to the base line. Flash photolysis of the unacetylated ZnPQ resulted in identical formation and decay kinetics for the ZnP^+Q^- state, but also present were long-lived transients that did not return to the base line (attributed to amine oxidation in the spacer units).

solvents a short-lived transient band was observed at 415 nm, with rise time (150 ns) clearly longer than the immediate formation of the porphyrin triplet state and decay time (1.4 μs) much faster than that of the triplet states of $ZnPQH_2(Ac)_4$ and $ZnPA_4(Ac)_4$ (>1 ms) (Figure 5). No transients ($\Delta A = 0$) at 415 nm were observed upon flashing $ZnPQH_2(Ac)_4$, establishing that 415 nm is an isosbestic wavelength for the triplet and the ground state.[24] The relatively slow growing in and fast decay observed upon flashing $ZnPQ(Ac)_4$ is therefore attributed to $ZnP^+Q^-(Ac)_4$. The 1.4-μs decay of $ZnP^+Q^-(Ac)_4$ fit a single exponential, indicating that the conformers PQ_a and PQ_b had equilibrated on this time scale. Unfortunately, the highly broadened spectra of both the triplet and radical cation of ortho-substituted tetraphenylporphyrins (see Experimental Section) make it difficult to distinguish these species spectroscopically (see below). The yield of the triplet state of $ZnPQ(Ac)_4$ in polar solvents is 0.25, and the yield of $ZnP^+Q^-(Ac)_4$ from the triplet state is unity.[26]

(25) Andrews, L. J.; Deroulede, A.; Linschitz, H. *J. Phys. Chem.* **1978**, *82*, 2304–2309.

(26) The triplet yield of $ZnPQ(Ac)_4$ is less than that of ZnTPP (Φ_T = 0.85) due to the singlet-state charge-transfer quenching process (Φ_{ET} = 0.60 in polar solvents). For Φ_T of ZnTPP, see: Hurley, J. K.; Sinai, N.; Linschitz, H. *Photochem. Photobiol.* **1983**, *38*, 9–14.

Table V. Triplet-State Reactions[a]

solvent	transient absorption, μs: rise of 415-nm band[b]	transient absorption, μs: decay at all wavelengths
	$ZnPQ(Ac)_4$	
toluene		90
dimethoxyethane		6.0
methyltetrahydrofuran		7.3
methylene chloride		1.4
acetonitrile	0.15	1.4
N,N-dimethylacetamide	0.15	1.4
propylene carbonate	0.15	1.2
	$ZnPQH_2(Ac)_4$	
ethanol/methanol (4:1)		3000

[a] At room temperature. [b] See Figure 5C.

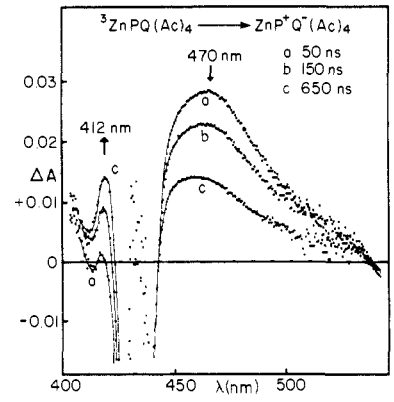

Figure 6. Difference spectra of $ZnPQ(Ac)_4$ in *N,N*-dimethylacetamide at increasing time points after excitation by a 13-ns laser pulse at 561 nm using the diode array spectrometer. The spectra show the decay of the triplet and $ZnP^+Q^-(Ac)_4$ (470 nm) and the rise in absorption of $ZnP^+Q^-(Ac)_4$ at 415 nm.

In nonpolar solvents, the 415-nm transient could not be observed, but the lifetime of the triplet state of $ZnPQ(Ac)_4$ was much shortened (Table V). In toluene, its lifetime was less than one-twentieth that of the triplet states of $ZnPQH_2(Ac)_4$ or $ZnPA_4(Ac)_4$. In solvents of intermediate polarity such as methyltetrahydrofuran, the 415-nm transient could not be observed but the transients exhibited greatly shortened lifetimes of only ~7 μs. The shortened lifetimes indicate that charge-transfer quenching interactions occur between the triplet state of the zinc–porphyrin and the quinone even in nonpolar solvents.

Difference spectra at various times following flash excitation of $ZnPQ(Ac)_4$ were collected by using a diode array pulsed spectrometer[27] with higher spectral resolution than the pulsed ruby apparatus (Figure 6). The kinetics of the absorbance changes in the 415- and 470-nm regions were similar to those measured with the pulsed ruby apparatus. The difference spectra at zero delay time were identical with the triplet spectra of the reference porphyrin $ZnPQH_2(Ac)_4$. During the first few 100 ns a growing in was observed in the 415-nm region, where the porphyrin cation absorbs more strongly than the triplet, and there was a small increase in absorbance just to the red of the bleached Soret band, where the cation has a strong absorbance as well. At longer delay times (1 μs) the difference spectra in the region 400–500 nm more closely matched that of the chemically produced $ZnPQ(Ac)_4$ cation than the triplet. Plots of ratios of absorbancy changes versus time at various wavelengths in the 400–600-nm region of the digital data from the diode array spectrometer clearly resolved small transients in the 100-ns time regime, confirming the formation of $ZnP^+Q^-(Ac)_4$ from the triplet state.[23]

Picosecond flash photolysis studies were performed on $ZnPQ(Ac)_4$ in an attempt to observe a P^+Q^- charge-separated state formed from the porphyrin excited-singlet state.[28] The por-

(27) Sedlmair, J.; Ballard, S. G.; Mauzerall, D. C. *Rev. Sci. Instrum.* **1986**, *57*, 2995–3003.

Table VI. Fluorescence Yields and Lifetimes of Free Base Porphyrins[a]

compd	rel ϕ_f	τ, ns	$k_f/10^7$,[b] s^{-1}
TPP[c]	1.0	9.8	1.33
$(o\text{-}H_2NPh)_4P$[d]	0.63	9.0	0.91
PQ	0.18	3.0	0.77
PA_4	0.18	3.2	0.75
$PQ(Ac)_4$	0.53	12.0	0.57
$PQH_2(Ac)_4$	0.45	12.2	0.48
$PA_4(Ac)_4$	0.56	12.5	0.58

[a] In acetonitrile at room temperature. The fluorescence lifetimes were single lifetimes to ~98%. [b] The fluorescence rate constants were calculated by taking the absolute fluorescence yield of TPP to be 0.13.[64] [c] In methylene chloride at room temperature. [d] *meso*-$\alpha,\alpha,\alpha,\alpha$-Tetrakis(*o*-aminophenyl)porphyrin.

phyrin–hydroquinone $ZnPQH_2(Ac)_4$ in acetonitrile/ethanol (3:1) at 0.1 ns showed a broad ΔA spectrum (440–540 nm) with peak at 465 nm. At 2.5 ns the absorption peak increased approximately 2-fold and sharpened slightly, becoming more characteristic of the triplet state observed at longer times with the photodiode array spectrometer. $ZnPQ(Ac)_4$, however, showed nearly identical ΔA spectra from 0.1 to 2.5 ns throughout the 440–540-nm range, with no observed increase in ΔA at 470 nm. Although the difference in ΔA behavior between $ZnPQ(Ac)_4$ and $ZnPQH_2(Ac)_4$ is striking, the very broad ΔA throughout the spectrum, the presence of several species [$^1ZnPQ(Ac)_4$, $^1ZnP^+Q^-(Ac)_4$, $^3ZnPQ(Ac)_4$] with similar spectra, and the expected biphasic kinetics on the nanosecond time scale due to the respective conformers make it difficult to unambiguously identify the formation and decay of the putative singlet $ZnP^+Q^-(Ac)_4$. However, no very short-lived flash transients were observed over the wavelength interval examined (370–650 nm) in flash photolysis experiments using the pulsed ruby or diode array spectrometers. Therefore, the lifetime of a $^1P^+Q^-$ charge-separated state must be less than the response times (30 ns) of these instruments.

Free Base Porphyrin–Quinones. The free base porphyrin–quinones are strikingly unreactive as compared with the zinc chelates (Table VI). The fluorescence decays of $PQ(Ac)_4$, $PQH_2(Ac)_4$, and $PA_4(Ac)_4$ follow single exponentials with essentially identical lifetimes; 12.2 ± 0.3 ns. This sets a minimum electron-transfer time of 400 ± 100 ns for the free base $PQ(Ac)_4$.

The lifetimes of the nonacetylated PQ and PA_4 are the same (3.1 ± 0.1 ns) but are only one-fourth that of their acetylated counterparts. The relatively low yields and shorter decay times found for both PQ and PA_4 cannot be attributed to interaction with oxidized quinone but do correlate with the presence of the benzylaniline groups. Nevertheless, the electron-transfer time constant of PQ must still be very long, >50 (± 20) ns. Flash photolysis of the free base $PQ(Ac)_4$ in *N*,*N*-dimethylacetamide at room temperature gave a long-lived triplet state (τ ~200 μs) with no observable radical ion state.

In contrast to the absence of electron-transfer interactions in the free base porphyrin–quinones, the singlet state of free base TPP was strongly quenched by added 2,3,5,6-tetramethoxy-1,4-benzoquinone in *N*,*N*-dimethylformamide at room temperature. The reaction followed good Stern–Volmer kinetics, with a bimolecular quenching rate constant $k_q = 6.4 \times 10^9$ M^{-1} s^{-1}. Benzoquinone and duroquinone also were effective quenchers, with $k_q = 6.8 \times 10^9$ and 4.1×10^9 M^{-1} s^{-1}, respectively.

Chlorin–Quinones. We sought to use the porphyrin–quinone as a means of examining the role of orbital symmetry in the electron-transfer process. Reduction of ZnTPP at one of the β-pyrrole positions forms a chlorin (C) and changes the molecular symmetry from D_{4h} to C_{2v}, thereby removing the degeneracy of the LUMOs of the zinc–porphyrin. Because a benzoquinone has D_{2h} symmetry, there are two possible structural isomers of cofacial chlorin–quinones (CQ). Ideally, one chlorin–quionone structural isomer would have the quinone carbonyl axis parallel to the symmetry axis of the chlorin, which bisects the reduced β-pyrrole bond, and the second chlorin–quinone isomer would have the quinone carbonyl axis perpendicular to the chlorin symmetry axis. The HOMO of the excited Zn–chlorin is symmetric about its unique axis containing the reduced pyrrole, and the LUMO of the quinone is symmetric about the carbonyl axis. Rapid forward and slow reverse electron transfer is expected in an isomer that contains these axes aligned, and slow forward but rapid reverse electron transfer in the isomer where these axes are perpendicular.

The synthetic routes of condensation of chlorin and quinone, and diimide reduction of PQ, both afforded the same two chlorin–quinone isomers, CQ-α and CQ-β (see Experimental Section). The amount of pure CQ-α and CQ-β that could be obtained was limited by the extreme difficulty of their separation by repetitive HPLC, thus precluding definitive assignments to the parallel and perpendicular isomeric structures.

Table VII. Fluorescence Yields and Lifetimes of Chlorin–Quinones[a]

compd	τ_1, ns	τ_2, ns	χ_1	rel ϕ_f[b]
ZnCQ-α	0.77	1.7	0.65	0.30
ZnCQ-β	0.55	2.0	0.85	0.19
CQ-α	3.1		1.0	0.33
CQ-β	3.1		1.0	0.33

[a] In acetonitrile/ethanol (5:1). Fluorescence yields were obtained by excitation at 410 nm (CQ) or 425 nm (ZnCQ) and determination of the fluorescence peak intensity at 660 nm (CQ) or 631 nm (ZnCQ). [b] The fluorescence yields of the zinc–chlorin–quinones are referenced to zinc–tetraphenylchlorin (ZnTPC, τ 1.30 ns), and the free base chlorin–quinones are referenced to tetraphenylchlorin (TPC, τ 5.0 ns). The lifetimes observed for ZnTPC and TPC cannot be used with certainty as values for τ_0 because of the *o*-amines in the chlorin–quinones. In the case of ZnCQ, the value of τ_2 can be used as an approximation of τ_0, given that τ_2 typically has a value very close to τ_0 in the zinc–porphyrin–quinones.

The fluorescence yields and lifetimes were identical for both the free base isomers (Table VII). However, the zinc chelates of CQ-α and CQ-β showed slightly different fluorescence yields, and each isomer showed biphasic fluorescence decay curves. These biphasic decays are attributed to the presence of two conformers, in analogy with the PQ case.[20] The small difference between the photochemical properties of ZnCQ-α and ZnCQ-β may be a result of the helical twisting of the quinone axis with respect to the chlorin, effectively rendering the chlorin–quinone orbital overlap similar in both ZnCQ-α and ZnCQ-β.

Acid Titration Experiments. We sought to use the porphyrin–quinone to explore the role of charged groups on the electron-transfer process. Conditions were found where the four benzylaniline groups in the zinc–porphyrins could be protonated without demetalation. Although the two lifetimes of ZnPQ changed little with acid concentration, the fraction of the fast component decreased continually with protonation, as measured by the sharpening of the Soret band. When fully protonated, $ZnPQ(H^+)_4$ shows only a single lifetime (τ 1.9 ns), and this lifetime and fluorescence yield are both identical with those of $ZnPA_4(H^+)_4$. The observed electron transfer in ZnPQ is thus inhibited by protonation.

Discussion

The PQ molecule is sufficiently complex that in addition to the usual external effects such as temperature and solvent, a variety of internal properties can be varied which affect the rate of electron transfer. Some of these properties such as symmetry, charge, and redox level were designed into the molecule. Others, such as the presence of two conformers kinetically distinct on the nanosecond time scale, were a serendipitous result of the molecular complexity. The data on temperature and distance dependence of the electron-transfer rates of the PQ derivatives provide strong evidence that the mechanism is that of electron tunneling. Effects of changing the bonding in PQ indicate that the tunneling is through space and not through bonds. The small effects of energetics and solvent variation support an interpretation of nonadiabatic electron tunneling. The effects of changing symmetry and of electrostatic

(28) Performed with Dr. Michael Wasielewski at Argonne National Laboratory.

(29) Guay, D.; Mauzerall, D. C., to be published.

charge, while less conclusive, are consistent with the tunneling mechanism. The complexity of the PQ molecule invites direct comparison with the bacterial reaction center.

Mechanism. The characteristics of electron transfer by electron–nuclear tunneling are that the transfer distance is greater than the sum of the van der Waals radii of the participating molecules and that the process has a small activation energy, approaching zero at low temperatures. The reactions of photoexcited $ZnPQ(Ac)_4$ show both of these characteristics.

The requirement for a small activation energy for electron transfer is clearly fulfilled in $ZnPQ(Ac)_4$ (Table IV). The electron transfer from the singlet state of PQ_a has an activation energy near 0 (±1.2 kJ/mol). Moreover, recent experiments in ethanol/methanol (4:1) show that the electron-transfer time of the PQ_a conformer *decreases* by a factor of 2 on cooling from 300 to 77 K, and the forward time constant of the triplet reaction increases 5-fold from 300 to 175 K (ΔE = 6.0 ± 1.3 kJ/mol).[23]

With regard to the transfer distance, the two porphyrin–quinone conformers, PQ_a and PQ_b, have estimated center-to-center distances of 6.5 and 8.5 Å, respectively, based on CPK models that conform to the NMR data.[20] The corresponding electron-transfer times, τ_a and τ_b, differ by approximately 5-fold for $ZnPQ(Ac)_4$ in polar solvents (Table III). The rate constant for electron transfer via tunneling is determined by the overlap of the wave functions of the donor and acceptor and will thus be a function of donor and acceptor distances, symmetries, and relative orientations in space.[12,22,30] The rate will vary exponentially with a suitable distance parameter, r_e, of the systems,[12] as shown in eq 8, where F is the Franck–Condon nuclear factor, γ is a frequency

$$\text{rate constant} = k = F\gamma\theta e^{-\alpha r_e} \qquad (8)$$

factor that is a mild function of the energy levels involved, θ is a function of the orientation of the π systems, and α is the tunneling parameter that contains the contribution to the tunneling probability of the intervening material between donor and acceptor. The observed difference between τ_a and τ_b in $ZnPQ(Ac)_4$ leads to a value for α of approximately 1.3 Å^{-1}. A similar value has been predicted earlier,[12] and several measurements on π aromatic donors and acceptors have given results of this magnitude.[31] Further discussion of mechanism is given below in the section on energetics.

Tunneling Through Space and Through Bonds. Mechanistic questions concerning intramolecular electron transfer in covalently linked donor–acceptor complexes have focused on the issue of "through-space" versus "through-bond" electron transmission pathways.[8,32] The inherent structural features of the ZnPQ molecule provide two tests of the relative importance of through-bond versus through-space conduction in this system. The four bridges of PQ have benzylaniline groups, which have a HOMO high in energy, are electron-rich, and are easily oxidized.[33] Acetylation lowers the energy of the HOMO and strongly increases the oxidation potential of the amine. However, acetylating the anilines in PQ to form acetanilides only decreased τ_a by 35% (Table III), and the triplet-state reactions of ZnPQ and $ZnPQ(Ac)_4$ occurred with identical rise and decay times of the P^+Q^- charge-separated state. The insensitivity of these electron-transfer processes in the zinc–porphyrin–quinones to gross changes in the bonding pathway provides evidence in favor of direct electron tunneling. The porphyrin–quinone containing Schiff base linkages in the spacer groups $ZnPQ(SB)_4$ also showed similar electron-transfer times, providing further support for direct electron tunneling.

A second argument in support of direct electron tunneling concerns the two conformers of PQ, which differ in intramolecular P–Q distance of separation. The fact that the two conformers differ in electron-transfer rate by a factor of 5 or more (attributed to a difference in distance) also suggests that through-bond is not the mechanism of transfer, because both conformers have the same bonds and very similar conformations along almost all the bonds.

The energy of the electron orbitals involved in the electron-transfer reactions of porphyrins, and in the photosynthetic reaction center, is low: <2 eV above the ground state. This factor alone strongly favors through-space electron transfer. The situation is very different for spacer-linked donors and acceptors with orbital energies of 5–6 eV,[32] where the electron energy is close enough to the energy levels of antibonding orbitals of the spacer atoms for them to be involved in through-bond transfer. We stress that the theory of the tunneling parameter α includes the polarizability of the intervening material and so includes the average of these empty orbitals in any case.[10,12]

It is noteworthy that the amine–porphyrin charge-transfer interactions of the nonacetylated compound ZnPQ have only a weak effect on the electron transfer to the quinone from either singlet or triplet states. This is because the aniline is an electron donor rather than an electron acceptor, and the aniline lone pair of electrons does not compete with the quinone for the occupied LUMO of the photoexcited porphyrin. The amine–porphyrin charge-transfer interactions in the free base PQ or PA_4 are more severe, diminishing the singlet-state lifetimes 4-fold (Table VI). This is expected because the excited-state free base porphyrin is a stronger electron acceptor than is the zinc chelate.[12]

Energetics. Currently accepted theories of electron transfer interpret a small temperature difference of the rate (at low temperature) in terms of nuclear tunneling. However, since the donor–acceptor distances in our porphyrin–quinone system are large, as noted, electron tunneling must occur, and we emphasize this aspect of the situation in our discussion.

Theories of electron-transfer reactions[34,41] describe the dependence of the rate constant on the energetics of the reaction and assign temperature dependence to the Franck–Condon factor (eq 8) as the overlap of the vibronic wave functions of the reactant and product. These in turn depend on the number and kinds of vibrational degrees of freedom in these molecules. The very large number of degrees of freedom in complex molecules (a quinone has some 30 vibrational modes and a porphyrin about 100) and the wide range of their frequencies result in a dense manifold once one is away from the zero-point levels. Particularly in condensed phase, relaxation from excited vibronic levels is very fast in complex molecules, and Stark broadening contributes further to the widths of energy levels, which approach the spacing of the low-frequency modes themselves. The result is a quasi-continuum of levels, which reduces the importance of Franck–Condon factors and ensures rapid trapping of the electron in the acceptor molecule. We estimate that it will require roughly about a full span of the vibrational modes (2000 cm^{-1}) above the zero-point levels to achieve this continuum. Thus, one may expect the electron-tunneling rate to actually decrease as the energy difference between the locally excited and electron-transferred states diminishes below this value (~0.25 eV). However, above this value the rate should become relatively insensitive to energy, if the free energy change in the reaction is favorable. Charge transfer to the quinone should favor formation of new lower frequency modes, thus adding a further entropy contribution to the transfer rate.[34]

The free energy change in a photoinduced electron transfer can be estimated by the expression $E^\circ = W^* + E(A^-) - E(D^+) + J$, where W^* is the electronic excitation energy of the donor (neglecting entropy effects on excitation), $E(A^-)$ is the reduction potential of the acceptor, $E(D^+)$ is the oxidation potential of the donor, and J is an electrostatic interaction free energy.[35] Though

(30) Cave, R. J.; Siders, P.; Marcus, R. A. *J. Phys. Chem.* **1986**, *90*, 1436–1444.

(31) For example, see: Heiler, D.; McLendon, G.; Rogalskyj, P. *J. Am. Chem. Soc.* **1987**, *109*, 604–606.

(32) Hush, N. S.; Paddon-Row, M. N.; Cotsaris, E.; Oevering, H.; Verhoeven, J. W.; Heppener, M. *Chem. Phys. Lett.* **1985**, *117*, 8–11. Beratan, D. N.; Onuchic, J. N.; Hopfield, J. J. *J. Chem. Phys.* **1985**, *83*, 5325–5329. Beratan, D. N.; Hopfield, J. J. *J. Am. Chem. Soc.* **1984**, *106*, 1584–1594. Oevering, H.; Paddon-Row, M. N.; Heppener, M.; Oliver, A. M.; Cotsaris, E.; Verhoeven, J. W.; Hush, N. S. *J. Am. Chem. Soc.* **1987**, *109*, 3258–3269. Ohta, K.; Closs, G. L.; Morokuma, K.; Green, N. J. *J. Am. Chem. Soc.* **1986**, *108*, 1319–1320.

(33) N. L. Weinberg, Ed. *Technique of Electroorganic Synthesis*, Part II; Wiley: New York, 1975; pp 807–826.

(34) Kakitani, T.; Kakitani, H. *Biochim. Biophys. Acta* **1981**, *635*, 498–514.

Table VIII. Redox and Excited-State Energetics of Porphyrin Derivatives

compd	W^*,[a] eV	$E(D^+)$[b]	$E°$	compd	τ_{ET},[c] ns
^{1}ZnTPC	2.03	0.60	0.76	^{1}ZnCQ	~1
^{1}ZnTPP	2.07	0.75	0.65	^{1}ZnPQ(Ac)$_4$	0.65
^{1}TPC	1.91	0.88	0.36	^{1}CQ	>8
^{1}PQ(Ac)$_4$	1.90	1.05	0.18	^{1}PQ(Ac)$_4$	>400
^{3}ZnTPP	1.59	0.75	0.17	^{3}ZnPQ(Ac)$_4$	150
^{3}TPP	1.45	1.05	−0.27	^{3}PQ(Ac)$_4$	>10^6

[a] The energy of the excited singlet or triplet states, measured by the 0–0 transitions of the fluorescence and phosphorescence bands, respectively. [b] All potentials are in volts and are referred to the saturated calomel electrode (SCE). $E° = W^* + E(A^-) - E(D^+)$, where $E(D^+)$ is the oxidation potential of the porphyrin or chlorin species, and $E(A^-)$ is the reduction potential of the quinone. The value for the quinone was taken from the reduction potential of 2,3,5,6-tetramethoxy-1,4-benzoquinone, $E(A^-) = -0.667$ V vs SCE, and literature values were used for the porphyrins[35] and the chlorins.[66] The actual potentials $E(D^+)$ and $E(A^-)$ of ZnPQ(Ac)$_4$ are both 0.1 V more positive than those quoted here (see Experimental Section), but $E°$ is not affected. [c] $\tau_{ET} = \tau_s$ for the singlet-state reaction and $\tau_{ET} = \tau$ for the triplet-state reaction.

the inherent errors in these estimations are ±0.1 V,[36] the overall energies of reaction can be used in a relative sense to compare the thermodynamic allowedness of photoinduced electron-transfer reactions among related compounds that differ in excited-state or redox energies (Table VIII).

The energetics of the porphyrin–quinone electron-transfer reactions are interpreted in Figure 7. The oxidation potential of the excited state $[E_{ox}^* = W^* - E(D^+)]$ of the various porphyrins is shown on the left in the figure, and the excess free energy $[\Delta E = W^* - E(D^+) + E(A^-)]$ for the charge-separation reaction with the quinone is shown on the right.

The relaxation energy for the change ZnP → ZnP$^+$ is very small, as measured by the nearly identical X-ray structures of ZnTPP and its radical cation salt,[37] but some relaxation energy is expected in passing from Q to Q$^-$, particularly in the C–O bond distance.[38] This is shown as a forbidden gap above the relaxed level of the semiquinone radical anion Q_r^-. The transfer occurs from P*Q to the state P$^+$Q$_u^-$, where the electron is bound in the unrelaxed Franck–Condon state of the semiquinone radical anion Q_u^-. Trapping follows tunneling by relaxation of Q_u^- to Q_r^-. The relaxation process $Q_u^- \rightarrow Q_r^-$ is considered here to include any solvent reorganization energy.

The level of Q_u^- in Figure 7 is chosen by the behavior of excited singlet free base PQ(Ac)$_4$ and triplet ZnPQ(Ac)$_4$, which have nearly identical $E°$ values (Table VIII). If this energy level lies close to the cutoff point, the reaction may or may not occur depending on slight effects of electronic state, temperature, or solvent. Thus, singlet PQ(Ac)$_4$ shows no reaction, while the observed electron-transfer reaction of triplet ZnPQ(Ac)$_4$ depends on both temperature and solvent (Table V). The relaxation energy thus obtained, $Q_u^- - Q_r^- \sim 0.2$ eV, is close to the value of ~0.3 eV estimated from bond distortions in quinones.[39] It is not ruled

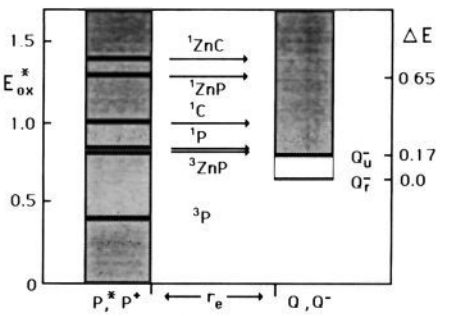

Figure 7. Energy levels for electron transfer in polar solvents. The excited-state oxidation potentials $[E_{ox}^* = W^* - E(D^+)]$ for the various porphyrin species are plotted as dark horizontal lines. The values used for the relaxed singlet- or triplet-state internal energies (W^*) and the oxidation potentials $[E(D^+)$ vs SCE] of the free base porphyrin (P), zinc porphyrin (ZnP), chlorin (C), and zinc chlorin (ZnC) are listed in Table VIII. The ΔE for the electron-transfer reaction $[\Delta E = W^* - E(D^+) + E(A^-)]$ is shown on the right-hand scale, where A^- is the reduction potential of the quinone. The actual potentials $E(D^+)$ and $E(A^-)$ of ZnPQ(Ac)$_4$ are both 0.1 V more positive than those shown (see Experimental Section). This does not change the ΔE but E_{ox}^* decreases 0.1 V. The stippling represents a continuum of energy levels extending upward from each of these states. The relaxation energy between P and P$^+$ is assumed to be negligible. The fixed energy level of Q_r^- is shown on the right. A significant relaxation energy (~0.2 eV) is shown in this case as a blank between the relaxed Q_r^- state and the unrelaxed Q_u^- formed by electron tunneling. The electrostatic term J is assumed negligible in polar solvents.

out that the allowed level is actually somewhat higher than the triplet ZnPQ(Ac)$_4$ level and the (negative) difference is the activation energy observed (~0.05 eV) for this reaction.

The energy available from the triplet PQ(Ac)$_4$ oxidation is insufficient for reaction, and none is observed within the several millisecond triplet lifetime. On the other hand, there is excess energy available for the reaction of singlet ZnPQ(Ac)$_4$ and the zinc–chlorins. These reactions are in fact observed, and that of singlet ZnPQ(Ac)$_4$ is largely independent of solvent (Table III) and temperature (Table IV). It is noteworthy that free tetramethoxyquinone quenches the fluorescence of free base TPP with a near encounter limited rate constant, $k_q = 6.4 \times 10^9$ M^{-1} s^{-1}. Similar differences between inter- and intramolecular quenching have been observed by Connolly et al.[40] This is readily explained by the distance dependence of electron transfer. In the porphyrin–quinone cage molecule the minimum edge-to-edge distance (r_e, eq 8) is ~3 Å in excess of the van der Waals distance, but in the solution encounter complex it may be near contact. Both forward and reverse reactions then become so fast that the ion products are not observed.[12] This is a good example of how a structured molecule can introduce specificity into a photochemical reaction.

It is of interest to test the applicability of an adiabatic theory[41] to these results. The (fast) electron-transfer times roughly track the $E°$ values (Table VIII). It is possible to fit the observed energies for both singlet and triplet reactions by assuming that $\lambda = -E° = 0.65$ eV for the singlet case. This leads to an activation energy of 0.08 eV for the triplet reaction compared with the observed 0.06 eV. However, the value $\lambda = 0.65$ seems an unreasonably high estimate of the quinone reorganization energy. Data on other porphyrin–quinone molecules have been fit with λ in the range 0.7–1.1 eV,[42] and even higher values, up to 1.3 eV, have been given.[39] Thus, this parameter seems to be quite arbitrary. Moreover, it is unlikely that this large value of λ rep-

(35) Seely, G. R. *Photochem. Photobiol.* **1978**, *27*, 639–654.

(36) $E°$ contains an electrostatic term to allow for the fact that electron transfer occurs at a finite distance, not the infinite dilution state of the redox potential. In fact, the redox potentials of organic molecules are usually obtained polarographically in polar organic solvents containing high concentrations of a supporting electrolyte. Thus, the electrostatic interactions may already contribute to the quoted potentials. Together with the approximation of equating Gibbs free energies of the redox potentials with internal energies of the excited states, the inherent errors in these estimations are large, ~0.1 V. See: Mauzerall, D.; Ballard, S. G. *Annu. Rev. Phys. Chem.* **1982**, *33*, 337–407.

(37) Spaulding, L. D.; Eller, P. G.; Bertrand, J. A.; Felton, R. H. *J. Am. Chem. Soc.* **1974**, *96*, 982–987.

(38) The C—O bond length of the semiquinone radical anion of benzoquinone is intermediate between that of the quinone (C═O, 1.224 Å) and hydroquinone (C—OH, 1.36 Å): "Tables of Interatomic Distances"; *Spec. Publ.—Chem. Soc.* **1958**, *No. 11*.

(39) Joran, A. D.; Leland, B. A.; Geller, G. G.; Hopfield, J. J.; Dervan, P. B. *J. Am. Chem. Soc.* **1984**, *106*, 6090–6092. Joran, A. D.; Leland, B. A.; Felker, P. M.; Zewail, A. H.; Hopfield, J. J.; Dervan, P. B. *Nature (London)* **1987**, *327*, 508–511.

(40) Connolly, J. S.; Hurley, J. K.; Bell, W. L.; Marsh, K. L. In *Photoinduced Charge Separation*; NATO ASI Series; V. Balzani, Ed.; Reidel: Dordrecht, The Netherlands, in press.

(41) $\Delta E^* = (E° + \lambda)^2(4\lambda)^{-1}$: Marcus, R. A.; Sutin, N. *Biochim. Biophys. Acta* **1985**, *811*, 265–322.

(42) Wasielewski, M. R.; Niemczyk, M. P.; Svec, W. A.; Pewitt, E. B. *J. Am. Chem. Soc.* **1985**, *107*, 1080–1082. Irvine, M. P.; Harrison, R. J.; Beddard, G. S.; Leighton, P.; Sanders, J. K. M. *Chem. Phys.* **1986**, *104*, 315–324.

resents solvation energy in view of the observed small solvent effect on the rate, as noted below. We propose that this small dependence of rate on $E°$ indicated by Table VIII may measure the change in density of energy levels involved in the nonadiabatic transition in the gap region.

Solvent Dependence. The relative yield of fluorescence of $ZnPQ(Ac)_4$ as a function of solvent (Table II) reflects changes in both the ratio of conformers PQ_a and PQ_b and the rate of electron transfer of each conformer. These two effects are readily separated by resolution of the biphasic fluorescence decay curves into components whose initial amplitudes indicate relative amounts of each conformer and whose lifetimes measure their rates of electron transfer.

The fast singlet-state electron-transfer time constant τ_a shows only a small dependence on solvent (Table III), decreasing only about 3-fold in passing from toluene (static dielectric constant, $\epsilon_s = 2.4$) to dimethyl sulfoxide ($\epsilon_s = 46.7$). Within the limits of a larger uncertainty, τ_b is also insensitive to the medium. These results are consistent with much data which showed that bimolecular quenching rate constants for both photoexcited and dark electron-transfer reactions of triplet-state porphyrins in solution were invariant to solvent static dielectric constant over a range of 2.5 to 110.[43]

For an electron-tunneling reaction, the overlap of the wave functions will be decreased by the presence of electrons in filled orbitals of intervening material (Pauli principle) but will be increased by the polarizability (electronic dielectric constant, determined by the separation of filled and unfilled orbitals).[12] Thus, one expects that it would be the optical dielectric constant ϵ_{op} not the static constant ϵ_s which partly determines the tunneling parameter α (eq 8) and that α should decrease with increasing polarizability of the intervening media. The present data do not clearly distinguish this effect, while that on other rigid porphyrin–quinones do show the expected dependence.[44]

The rather small solvent effects in these systems may be interpreted as possible solvent-dependent structural changes, which would influence the P–Q distance. Table III shows that those solvents with an equilibrium constant between the conformers of $K \simeq 1$ have $\tau_b/\tau_a \simeq 5$, while those solvents favoring PQ_a over PQ_b ($K \simeq 5$) have $\tau_b/\tau_a \simeq 20$. Thus, those solvents that favor the compact conformer PQ_a (large K) also show lower values of τ_a. By use of eq 8 with $\alpha = 1.5$ A^{-1}, the τ_b/τ_a ratios translate into differential distances of $\simeq 1$ Å (ethyl acetate, acetonitrile) and $\simeq 2$ Å (ethanol, dimethylacetamide), respectively. The size of the cavity in PQ is sufficiently large to host several small solvent molecules. Space-filling models show that one molecule of toluene, for example, can freely fit inside PQ_a and two molecules of toluene can fit in a face-to-face arrangement in PQ_b. With space available, these solvent groupings may reflect different cavity-packing modes, perhaps associated with different internal pressures characteristic of each solvent.[45] The solvent sensitivity of τ_b for the conformer with largest P–Q separation is in accord with this interpretation. Along with any solvent-dependent distance change, the relative orientation of the porphyrin and quinone rings will also vary because of the helical movement of the groups and this rotation will also modify electron overlap and the rate of electron transfer.[46]

The observed small increase in τ_a for singlet $ZnPQ(Ac)_4$ in passing from polar (dimethylacetamide) to nonpolar (toluene) media (Table III) may be assigned to a slight increase in the energy of the dipolar P^+Q^- state. One can estimate the *difference* in redox energy of the P^+Q^- radical ion pair in polar solvents versus that in toluene by the Onsager dipole cavity energy.[47] For a unit charge separation of 5 Å in a cavity of 7 Å radius, the energy difference is 0.4 eV. The number can be increased by a factor of 2 if the dipole length is increased to 7 Å or decreased by a factor of 2 by a small increase in the dielectric constant of the cavity. This is sufficient to raise the tunneling level (i.e., that of Q_u^-) close to that of singlet $ZnPQ(Ac)_4$, thus slowing the reaction. We reserve a more detailed discussion of mechanism and comparison with theories for a subsequent paper containing further details of solvent and temperature effects.[23]

The shortened triplet lifetime of $ZnPQ(Ac)_4$ in all solvents (Table V) is attributed to quenching by electron transfer. The absence of evidence for a charge-separated state in nonpolar and slightly polar solvents is caused by either the short lifetime of this state or insufficient spectral resolution[23] between this state and the triplet. In any case, the transient P^+Q^- states must live long enough (~ 1 ns) for spin dephasing to occur, allowing decay to the ground state.[48]

Symmetry. In a tunneling mechanism of electron transfer the rate is partly determined by the overlap of the donor and acceptor molecular orbitals. In addition to the edge-to-edge distance, the symmetry of the donor and acceptor molecular orbitals and their respective spatial orientations will be important in determining the overlap. In the porphyrin–quinone the photoinduced forward electron-transfer reaction occurs between the porphyrin LUMO and the quinone LUMO. The dark reverse electron transfer occurs between the quinone LUMO and the porphyrin HOMO. These differences in frontier orbital symmetries may be one source of rate differentials in forward and reverse electron-transfer processes.[49]

The free base chlorin–quinone isomers have identical fluorescence yields and identical monophasic lifetimes. Therefore, the electron-transfer times must be slow, as in the case of the corresponding free base porphyrin–quinone. However, the zinc-chlorin–quinones (ZnCQ, Table VII) each exhibit two lifetimes, but with only a slight difference between the two isomers. An explanation of these small differences is that both conformers of each chlorin–quinone structural isomer have the quinone rotated close to 45° with respect to the chlorin N–N axes because of the helical twisting of the four bridging groups, as occurs in PQ. While the slight difference between isomers favors the symmetry argument, we do not have independent evidence for the structure of the isomers.

Charge Effects. It is expected that appropriately positioned charges would facilitate the forward electron transfer and hinder the reverse transfer through electrostatic interactions. A positive charge placed on the other side of an acceptor (DA^+), or a negative charge by a donor (^-DA), or both would favor charge separation. Rackovsky and Scher have calculated the effect of charges on the rate of electron transfer and have shown that enhancement by an order of magnitude is possible.[50] An example may occur in the bacterial reaction center involving the ferrous ion close to the quinone acceptor.

It was expected that the effect in ZnPQ might be small because charge on the aniline groups would be close to the midplane between the porphyrin and quinone. In fact, the short lifetime did not change with protonation, but the fraction of short-lived fluorescence decreased in proportion to protonation.[29] One interpretation is that protonation causes a conformational change, forming entirely PQ_b or possibly a nontwisted, upright conformer that is not photochemically active on the nanosecond time scale due to a large P–Q distance of separation. It is evident that in other structures protonation may have the opposite effect, leading to conformational changes that favor more rapid electron transfer.

Comparison with Reaction Centers. A comparison between the properties of the porphyrin–quinone system [$ZnPQ(Ac)_4$] and those of the bacterial reaction center is instructive. Both are stable and capable of many operational cycles with no measurable side reactions. Both involve long-distance, weakly temperature-dependent electron transfer although the distance in the reaction

(43) Ballard, S. G.; Mauzerall, D. C. *J. Chem. Phys.* **1980**, *72*, 933–947. Ballard, S. G.; Mauzerall, D. C. *Biophys. J.* **1978**, *24*, 335–345.
(44) Leland, B. A.; Joran, A. D.; Felker, P. M.; Hopfield, J. J.; Zewail, A. H.; Dervan, P. B. *J. Phys. Chem.* **1985**, *89*, 5571–5573.
(45) Hildebrand, J. *Proc. Phys. Soc., London* **1944**, *56*, 221–239.
(46) Pietro, W. J.; Marks, T. J.; Ratner, M. A. *J. Am. Chem. Soc.* **1985**, *107*, 5387–5391. Gutfreund, H.; Weger, M. *Phys. Rev. B.: Solid State* **1977**, *16*, 1753–1755.
(47) Onsager, L. *J. Am. Chem. Soc.* **1936**, *58*, 1486–1493.
(48) Periasamy, N.; Linschitz, H. *Chem. Phys. Lett.* **1979**, *64*, 281–285.
(49) Mauzerall, D. In *Photoinduced Electron Transfer*; Fox, M. A., Chanon, M., Eds.; Elsevier: Amsterdam, in press.
(50) Rackovsky, S.; Scher, H. *Biochim. Biophys. Acta* **1982**, *681*, 152–160.

center is far larger (30 vs 7 Å). The quantum yield of charge separation in the reaction center is ≥0.95.[51] For $ZnPQ(Ac)_4$ in polar solvents charge transfer is also the predominant reaction pathway, giving about 60% quantum yield from the singlet and unity quantum yield from the triplet ($\phi_T \sim 0.25$). The lifetime of the charge-separated state in the reaction center is much greater (>30 ms) than that of triplet $ZnP^+Q^-(Ac)_4$ (1 μs). The lifetime of singlet $ZnP^+Q^-(Ac)_4$ remains undetermined. The free energy storage in the reaction center is ~0.5 eV,[52] while that in $ZnPQ(Ac)_4$ is ~1.4 eV based on the triplet-state reaction. Since the reduction potentials of the quinone in the model and in the reaction center are similar, the higher energy yield in the porphyrin–quinone derives from the higher oxidation potential of the porphyrin over that of the bacteriochlorin. It is only on this last point that one has exceeded Nature's product.

Conclusion. Electron transfer occurs from porphyrin excited states in a synthetic, cofacial porphyrin–quinone cage molecule linked by appropriate spacers at a P–Q distance of about 7 Å. The distance and temperature dependence of this reaction indicates that it occurs via through-space nonadiabatic electron tunneling. Studies of the effects of solvents, changes in symmetry, and added charges are consistent with this interpretation. The PQ molecule is sufficiently complex that conformational change affects its reactivity.

Experimental Section

General Procedures. All samples of ZnPQ, $ZnPA_4$, $ZnPQ(Ac)_4$, $ZnPA_4(Ac)_4$, CQ, and ZnCQ were purified by HPLC prior to photochemical and spectroscopic analyses. High-pressure liquid chromatography was performed on silica gel columns (Waters Associates). Nonpolar solvents such as hexane/ethyl acetate were used to elute the unacetylated porphyrins. More polar solvents such as ethyl acetate containing a few percent methanol were used for chromatography of the acetylated porphyrins.

Mass spectral analysis was performed by ^{252}Cf fission fragment mass spectrometry.[53] Samples of approximately 20 μg of porphyrin in acetone or chloroform/methanol were electrosprayed onto aluminized polyester. Positive ion spectra were collected in 1–30 min. Cage porphyrins[13] and substituted tetraphenylporphyrins[54] generally produce intense parent molecular ions in this method. The calculated average molecular weight (formula weight) and the most intense peak observed in the parent ion cluster are reported for each compound. Because most of the porphyrins described in this paper have more than 100 atoms, the isotopic distribution of parent ions typically encompasses several mass units. The presence of zinc, which has five important isotopes of natural occurrence, further broadens the distribution.

Zn–Porphyrins. The PQ and PA_4 compounds were characterized by HPLC, ^1H NMR, and UV–vis spectroscopy and ^{252}Cf fission fragment mass spectrometry.[13] Samples of PQ and PA_4 were converted to the zinc derivatives by addition of methanolic zinc acetate in excess to the free base porphyrins in CH_2Cl_2 at room temperature. Metalation usually occurred quantitatively within a few minutes. Gentle warming of the solution was required with concentrated samples. The disappearance of the free base porphyrin was monitored by absorption and fluorescence excitation and emission spectroscopy. The Zn–porphyrin was worked up by washing with 5% aqueous $NaHCO_3$, followed by passage over a short silica column to remove residual zinc acetate.

Amide Porphyrin Derivatives. The progress of the amidation reaction was followed by the sharpening of the Soret band in the absorption spectrum, by HPLC, and by mass spectral analysis. To a solution of ZnPQ (0.2 mM) in chloroform at room temperature was added excess acetic ahydride (0.18 M). Removal of an aliquot during the course of the reaction followed by ^{252}Cf fission fragment mass spectral analysis showed a cluster of peaks: MS (assignment, relative percent of total ions in cluster) 1523.5 ($ZnPQ(Ac)_2 + H^+$, 13), 1565.3 ($ZnPQ(Ac)_3 + H^+$, 22), 1587.6 ($ZnPQ(Ac)_3 + Na^+$, 16), 1605.9 ($ZnPQ(Ac)_4^{\cdot+}$, 20), 1629.7 ($ZnPQ(Ac)_4 + Na^+$, 29). HPLC analysis of the reaction mixture was performed on a silica column. The initial eluant of hexane/ethyl acetate (1:1) eluted ZnPQ. A step gradient terminating with ethyl acetate containing 5% methanol was used to elute the acetylated porphyrin compounds. The Soret band steadily increased in intensity and narrowed in width over the course of the reaction (Figure 2). The visible bands were nearly identical in ZnPQ and $ZnPQ(Ac)_4$. The acetylation reaction was allowed to proceed overnight. Excess acetic anhydride was removed by evaporation, and the crude porphyrin product was purified by semipreparative HPLC (silica, ethyl acetate/2% methanol). The $ZnPQ(Ac)_4$ product was obtained in 80% yield. $ZnPQ(Ac)_4$, $C_{94}H_{76}N_8O_{14}Zn$ (1607.1): calcd M 1604.5; obsd 1607.2 $(M + H)^+$, 1629.7 $(M + Na)^+$. The sodium addition complex was observed at an intensity 2.7 times that of the parent ion. The same procedure was used in the acetylation of $ZnPA_4$. $ZnPA_4(Ac)_4$, $C_{84}H_{72}N_8O_8Zn$ (1386.9): calcd M 1384.5; obsd 1385.7 $(M + H)^+$, 1409.5 $(M + Na)^+$.

The free base amide porphyrins $PQ(Ac)_4$ and $PA_4(Ac)_4$ were prepared by demetalation of the parent zinc complexes, after the latter were purified by HPLC and characterized. Demetalation to regenerate the free base porphyrin was achieved by adding excess trifluoroacetic acid to the zinc–porphyrin in CH_2Cl_2. After being stirred for 10–30 min, the green solution was washed with 10% $NaHCO_3$, dried (Na_2SO_4), and concentrated. The disappearance of the zinc porphyrin was confirmed by absorption and fluorescence excitation and emission spectroscopy. The purity of the products was established by HPLC.

Absorption Spectral Parameters. In CH_2Cl_2/ethanol (7:3), listed as compound, λ (nm) (ε M^{-1} cm^{-1}, fwhm nm): PQ, 286 (35400), 414 (124400, 40), 518 (12400), 556 (3100), 592 (4100), 649 (700); ZnPQ, 286 (37100), 429 (172000, 27), 522 (2930), 558 (16200, 22.4), 598 (3300); $ZnPQ(Ac)_4$, 304 (27300), 430 (455000, 10.2), 521 (3000), 561 (18500, 21.3), 598 (3700); ZnTPP, 423 (563000, 9.0), 555 (15300, 21.0), 594 (4900); Zn-5-(2-aminophenyl)-10,15,20-triphenylporphyrin,[55] 424 (501000, 10.2), 555 (17300, 21.2), 595 (5300); Zn-*meso*-α,α,α,α-tetrakis(*o*-aminophenyl)porphyrin, 425 (262000, 14.5), 555 (14400, 22.2), 593 (2700). The visible absorption spectra of ZnPQ and $ZnPA_4$ are nearly identical, as are those of $ZnPQ(Ac)_4$ and $ZnPA_4(Ac)_4$. The ortho-substituted porphyrins show characteristic phyllo-type spectra.[56]

Porphyrin Hydroquinones. The porphyrin hydroquinones were prepared in situ in protonic solvents such as acetonitrile/ethanol (3:1), *N*,*N*-dimethylacetamide/ethanol (1:1), or methanol/ethanol (4:1). To a cuvette containing an ethanolic solution of PQ was added an aliquot of ethanolic $NaBH_4$ (0.66 M stock solution) to give a final concentration of ~4 mM $NaBH_4$. Conversion to the hydroquinone (PQH_2) was verified in several instances by HPLC and mass spectral analysis. PQH_2, $C_{86}H_{72}N_8O_{10}$ (1375.6): calcd M 1376.4; obsd 1377.6 $(M + H)^+$. The reaction could be reversed by oxidation. To a sample of PQH_2 in DMF (2 mL) was added 0.1 mL of 0.46 M aqueous $K_3Fe(CN)_6$. Additional H_2O was added to produce a homogeneous solution. After 1 h the solution was extracted with toluene and analyzed by HPLC, giving a product composition of 81% PQ and 19% unreacted PQH_2.

Porphyrin Radical Cations. Addition of a 10-μL aliquot of 1 mM $Fe(ClO_4)_3$ to a solution of $ZnPQ(Ac)_4$ in CH_3CN (2.5 μM) gave quantitative conversion to the porphyrin radical cation. When 10 μL of triethylamine was added to the $ZnPQ(Ac)_4^{\cdot+}$ solution, the Soret band was restored to 86% of its original magnitude, indicating near quantitative regeneration of the neutral closed-shell porphyrin. This regeneration reaction failed with porphyrins bearing *o*-aminophenyl moieties, such as ZnPQ and Zn-*meso*-α,α,α,α-tetrakis(*o*-aminophenyl)porphyrin.

The radical cation of $ZnPQ(Ac)_4$ has a very broad, featureless absorption spectrum (ε >10,000 M^{-1} cm^{-1} from 350 to 490 nm): [λ (nm) (ε M^{-1} cm^{-1})], 413 (70000), 470 (27300), 650 (4000). The Δε [extinction of $ZnPQ(Ac)_4^{\cdot+}$ minus extinction of $ZnPQ(Ac)_4$] at 415 nm = 16000 M^{-1} cm^{-1}. This is to be compared with $ZnTPP^{\cdot+}$, which has $\epsilon_{409\,nm}$ 190000 M^{-1} cm^{-1} and $\epsilon_{650\,nm}$ 10000 M^{-1} cm^{-1}.[18] We confirmed these data for $ZnTPP^{\cdot+}$ in CH_3CN by oxidation of ZnTPP with $Fe(ClO_4)_3$. The absorption spectrum of $ZnTPP^{\cdot+}$ shifted only slightly: λ_{max} 406 nm, ε 177000 M^{-1} cm^{-1}; $\Delta\epsilon_{406\,nm} \cong 130000$ M^{-1} cm^{-1}.

Chlorin–Quinones. Two separate procedures were employed to prepare the chlorin–quinones, the condensation of *meso*-α,α,α,α-tetrakis(*o*-aminophenyl)chlorin with the quinone tetraaldehyde and the direct conversion of PQ to the chlorin–quinones CQ. Both procedures required difficult chromatography to separate the chlorin–quinone structural isomers.

A sample of 15 mg of *meso*-α,α,α,α-tetrakis(*o*-aminophenyl)-porphyrin[57] was dissolved in 15 mL of tetrahydrofuran, and aliquots of

(51) Wraight, C. A.; Clayton, R. K. *Biochim. Biophys. Acta* **1974**, *333*, 246–260.
(52) Woodbury, N. W.; Parson, W. W.; Gunner, M. R.; Prince, R. C.; Dutton, P. L. *Biochim. Biophys. Acta* **1986**, *851*, 6–22.
(53) Chait, B. T.; Agosta, W. C.; Field, F. H. *Int. J. Mass. Spectrom. Ion Phys.* **1981**, *39*, 339–366.
(54) Lindsey, J. S.; Schreiman, I. C.; Hsu, H. C.; Kearney, P. C.; Marguerettaz, A. M. *J. Org. Chem.* **1987**, *52*, 827–836.
(55) Collman, J. P.; Brauman, J. I.; Doxsee, K. M.; Halbert, T. R.; Bunnenberg, E.; Linder, R. E.; LaMar, G. N.; Del Gaudio, J.; Land, G.; Spartalian, K. *J. Am. Chem. Soc.* **1980**, *102*, 4182–4192.
(56) Falk, J. E. *Porphyrins and Metalloporphyrins*; Elsevier: New York, 1964; pp 72–80. Kim, J. B.; Leonard, J. J.; Longo, F. R. *J. Am. Chem. Soc.* **1972**, *94*, 3986–3992. Meot-Ner, M.; Adler, A. D. *J. Am. Chem. Soc.* **1975**, *97*, 5107–5111.

potassium azodicarboxylate[58] and glacial acetic acid were added over the course of 24 h. By use of the extinction coefficients of tetraphenylporphyrin, tetraphenylchlorin, and tetraphenylbacteriochlorin at 520, 650, and 740 nm,[59] the distribution of components was estimated to be 26% porphyrin, 67% chlorin, and 7% bacteriochlorin. Medium-pressure preparative liquid chromatography (silica, methylene chloride/ethyl acetate 1:2) afforded 5.4 mg of *meso*-$\alpha,\alpha,\alpha,\alpha$-tetrakis(*o*-aminophenyl)-chlorin (36% yield). No other atropisomers were present, and the chlorin was contaminated with less than 1% of porphyrin and bacteriochlorin species.

Equimolar amounts of *meso*-$\alpha,\alpha,\alpha,\alpha$-tetrakis(*o*-aminophenyl)chlorin and the quinone tetraaldehyde were condensed at 5×10^{-4} M in dimethyl sulfoxide containing 4×10^{-3} M trifluoroacetic acid.[13] HPLC analysis on silica gel showed two partially resolved peaks together accounting for 25% of the yield of product. Mass spectral analysis of the fraction consisting of both peaks showed the presence of the chlorin–quinone cage molecules. CQ, $C_{86}H_{72}N_8O_{10}$ (1377.6): calcd M 1376.4; obsd 1377.8 $(M + H)^+$. HPLC using hexane/ethyl acetate (2.5:1, 1 mL/min) enabled the two peaks to be resolved sufficiently well that relatively pure components could be obtained upon repetitive separation. Both components exhibited identical parent ion peaks and very similar fragmentation patterns upon mass spectral analysis. The visible absorption spectra and fluorescence emission spectra of both components were also identical, resembling that of tetraphenylchlorin:[60] CQ, λ_{abs} 405, 415, 652 nm, λ_{em} 660, 725 nm; ZnCQ, λ_{abs} 425, 626 nm, λ_{em} 631, 688 nm. The long-wavelength emission band (688 or 725 nm) was quite weak in both compounds.

A more expeditious synthesis involved the direct conversion of PQ to the chlorin–quinones. A sample of PQ was dissolved in tetrahydrofuran, and aliquots of potassium azodicarboxylate and glacial acetic acid were added over the course of 24 h at room temperature. The insoluble salts were removed, and the crude products in tetrahydrofuran were treated with MnO_2 to oxidize hydroquinone species to the corresponding quinones. Preparative HPLC as described above afforded a 75% yield of chlorin–quinones in roughly a 2:3 ratio of the two chlorin–quinone structural isomers. Further chromatography afforded the two chlorin–quinone structural isomers in greater than 95% isomeric purity. These chlorin–quinones cochromatographed with the chlorin–quinones obtained by condensation. No porphyrin or bacteriochlorin species could be detected in the chlorin–quinone fractions by absorption spectroscopy.

Electrochemistry. Cyclic voltammetry of $ZnPQ(Ac)_4$ gave $E_{ox}(CH_2Cl_2) = +0.95$ V and $E_{red}(DMF) = -0.44$ V (vs Ag/AgCl electrode with 0.1 M tetra-*N*-butylammonium perchlorate as supporting electrolyte). Under these same conditions, ZnTPP gave $E_{ox}(CH_2Cl_2) = +0.835$ V, and 2,3,5,6-tetramethoxy-1,4-benzoquinone[61] gave $E_{red}(DMF) = -0.52$ V (performed by Michael Atamian at Carnegie Mellon University).

Cyclic voltammetry of 2,3,5,6-tetramethoxy-1,4-benzoquinone was also performed in CH_3CN with tetra-*N*-butylammonium perchlorate as supporting electrolyte and a hanging mercury drop measuring electrode. Average values (five analyses) of -667 ± 4 and -1310 ± 10 mV (vs saturated calomel electrode) were obtained for the two transitions (performed by Dr. Paul Loach at Northwestern University). Also see ref 62.

Fluorescence Spectroscopy. Fluorescence yields were measured by the integrated yield of the two emission bands (near 610 and 660 or 650 and 720 nm) of the porphyrin compounds. The ratio of the two emission bands changed upon substitution at the ortho positions. The ratios are listed as compound, 610/660 ratio of integrated emission: ZnTPP, 0.94; ZnPQ, 0.59; $ZnPA_4$, 0.57; $ZnPQH_2$, 0.66; $ZnPQ(Ac)_4$, 0.45; $ZnPQH_2(Ac)_4$, 0.47; $ZnPA_4(Ac)_4$, 0.48; $ZnPQ(SB)_4$, 0.67. For the free base compounds, 650/720 ratio of integrated emission: TPP, 2.4; tetrakis(*o*-aminophenyl)porphyrin, 1.42; $PQ(SB)_4$, 1.41; PQ, 1.18; PA_4, 1.17.

Fluorescence lifetimes were measured by using a 300-ps pulse at 337 nm from a N_2 laser (PRA Nitromite LN100) or the output of a dye laser pumped by a N_2 laser, a microchannel plate photomultiplier (Hamamatsu R1294-01), a scan converter digitizer (Tektronix 7912AD), and a computer (Hewlett-Packard 9825A). Typically, 64–128 data sets were collected at 2 Hz for one fluorescence decay. Fluorescence lifetimes were measured at two wavelengths, 610 and 660 nm, with notch filters. Fluorescence decays were fitted by iterative deconvolution.[63] The resulting residuals show that the rise and decay are well fitted, with only high-frequency, low-amplitude noise remaining (Figure 4). The error in determining a lifetime was ±0.04 ns. At 337 nm the porphyrin absorbs much more strongly than does the quinone. Tetramethoxy-*p*-benzoquinone has absorption bands at 302 nm (ϵ 17 000 M^{-1} cm^{-1}) and 400 nm (ϵ 263 M^{-1} cm^{-1}) but absorbs only weakly at 337 nm (ϵ 156 M^{-1} cm^{-1}). The compound ZnPQ has $\epsilon_{337\,nm}$ 11 600 M^{-1} cm^{-1}.

The sample cell for the low-temperature fluorescence measurements was a long-necked, 1-cm^2 quartz fluorescence cuvette (Precision Cells). The temperature of the sample was controlled by a liquid N_2 cooled cryostat (Oxford Systems Inc.). The cryostat and regulating circuit have a temperature drift of less than 1 K over a 15–20-min span. The sample was allowed to equilibrate at each temperature for 10 min. No hysteresis was detected. Sample concentrations were $\leq 2 \times 10^{-6}$ M. The concentration of O_2 in each sample was reduced by bubbling N_2 into the sample cell for 10 min prior to the experiment. No degradation of samples of $ZnPQ(Ac)_4$ following fluorescence lifetime measurements was detected upon examination by absorption spectroscopy and HPLC.

Flash Photolysis. Flash photolysis measurements were carried out with both a pulsed ruby apparatus[25] and a diode array pulsed spectrometer.[27] The pulsed ruby apparatus utilized a Q-switched ruby laser frequency doubled to 347 nm with 30-ns resolution and 4–6-nm bandwidth measuring source. Sample concentrations were 2–50 μM with $A_{347\,nm}$ of ~0.02–0.52. The diode array pulsed spectrometer has 20-ns resolution with spectral resolution of 2 nm over a range of 200 nm. Excitation was by a 13-ns pulse at 561 nm (1 mJ) from an Xe–Cl excimer pumped dye laser (Lamda Physik 50E, FL-2000). A pulsed N_2 laser (Molectron UV1000) was used to excite a mixture of Coumarin 440, PPO, and Rhodamine 590 in methanol, and the resulting broad-band fluorescence was used as the measuring pulse. Data acquisition and analysis was done with a DATA 6000 digitizer (Analogic) and a HP86 computer (Hewlett-Packard). Porphyrin solutions at 2–10 μM concentrations were deoxygenated by a stream of pure nitrogen in a metal and glass coaxial flow system. Each difference spectrum was typically the collected average of 64–128 data sets.

Acid Titration Experiments. Amino porphyrins (ZnPQ, $ZnPA_4$) in CH_2Cl_2/ethanol (7:3) containing 0.44 M tetra-*N*-butylammonium perchlorate were titrated with trifluoroacetic acid. The titration was monitored by the sharpening of the Soret band and decrease of the aniline n–π^* transitions (296 nm); the spectral changes were complete upon reaching 1.4 M trifluoroacetic acid. The resulting absorption spectra were essentially identical with those of the acetylated porphyrins, indicating formation of $ZnPQ(H^+)_4$ and $ZnPA_4(H^+)_4$ (Figure 2). Though ZnTPP was instantly demetalated under these conditions, the *o*-amino porphyrins were rather stable (<10% demetalation over 2 h). The spectral properties of the porphyrins in neutral solution were unaltered in the presence of the supporting electrolyte.

Acknowledgment. This research was supported by grants from the NSF-DMB (83-16373), NIH (GM25693), and Rockefeller University Student Program and from the U.S. Department of Energy, Division of Chemical Sciences, Office of Basic Energy Sciences (Grant 84ER13223), to Brandeis University. The fission fragment mass spectrometric analyses were performed by Brian Chait of The Rockefeller University Mass Spectrometric Research Resource supported by the Division of Research Resources, NIH. We thank Michael Atamian and Dr. Paul Loach for performing electrochemical measurements and Dr. Michael Wasielewski for picosecond flash photolysis measurements.

(57) Collman, J. P.; Gagne, R. R.; Reed, C. A.; Halbert, T. R.; Lang, G.; Robinson, W. T. *J. Am. Chem. Soc.* **1975**, *97*, 1427–1439. Lindsey, J. S. *J. Org. Chem.* **1980**, *45*, 5215.

(58) Berson, J. A.; Poonian, M. S.; Libbey, W. J. *J. Am. Chem. Soc.* **1969**, *91*, 5567–5579. Hamersma, J. W.; Snyder, E. I. *J. Org. Chem.* **1965**, *30*, 3985–3988.

(59) Whitlock, H. W.; Hanauer, R.; Oester, M. Y.; Bower, B. K. *J. Am. Chem. Soc.* **1969**, *91*, 7485–7489.

(60) Dorough, G. D.; Huennekens, F. M. *J. Am. Chem. Soc.* **1952**, *74*, 3974–3976.

(61) Verter, H. S.; Rogers, J. *J. Org. Chem.* **1966**, *31*, 987–988. Wallenfels, K.; Friedrich, K. *Chem. Ber.* **1960**, *93*, 3070–3082.

(62) Flaig, W.; Beutelspacher, H.; Riemer, H.; Kälke, E. *Justus Liebigs Ann. Chem.* **1968**, *719*, 96–111. Bessard, J.; Cauquis, G.; Serve, D. *Electrochim. Acta* **1980**, *25*, 1187–1197.

(63) Mauzerall, D. C. *Biochim. Biophys. Acta* **1985**, *809*, 11–16.

(64) Harriman, A.; Porter, G.; Searle, N. *J. Chem. Soc., Faraday Trans. 2* **1979**, *75*, 1515–1521.

(65) $ZnPA_4(Ac)_4$ and $ZnPQH_2(Ac)_4$ in degassed ethanol/methanol (4:1) gave $\tau = 2.35$ ns at room temperature and $\tau = 2.50 \pm 0.06$ ns from 173 to 83 K. The values of τ_1 in $ZnPQ(Ac)_4$ were unaffected by the presence of O_2, but the τ_2 values were shortened slightly. The value of 2.5 ns was used for τ_0 for all calculations of τ_a and τ_b in $ZnPQ(Ac)_4$.

(66) Chang, C. K.; Hanson, L. K.; Richardson, P. F.; Young, R.; Fajer, J. *Proc. Natl. Acad. Sci. U.S.A.* **1981**, *78*, 2652–2656.